Sedimentology (2005) **52,** 1229–1252 doi: 10.1111/j.1365-3091.2005.00739.x

Genesis of large siliceous stromatolites at Frying Pan Lake, Waimangu geothermal field, North Island, New Zealand

BRIAN JONES*, ROBIN W. RENAUT† and KURT O. KONHAUSER*
**Department of Earth and Atmospheric Sciences, University of Alberta, Edmonton, Alberta, Canada, T6G 2E3 (E-mail: brian.jones@ualberta.ca)*
†Department of Geological Sciences, University of Saskatchewan, Saskatoon, Saskatchewan, Canada, S7N 5E2

ABSTRACT

Lilypad stromatolites, up to 3 m long and 1·5 m wide, were found to be actively growing in the shallow marginal waters of Frying Pan Lake and its outflow channel. These stromatolites, composed of *Phormidium* (> 90%), *Fischerella*, and a variety of other microbes, develop through a series of distinct growth stages. Dark green microbial mats cover the floor of the outflow channel and give rise to columns of various sizes and shapes in the shallower marginal waters. Once the columns reach the water level, the mats spread laterally to form a lilypad stromatolite. The lilypads are characterized by a raised, dark green rim, 4–5 mm high, that encircles a flat interior covered with a distinctive orange-red mat. The microbes forming the columns and lilypad plate are being actively silicified. The stromatolites are formed of: (i) flat-lying *Phormidium* filaments (P-laminae), (ii) upright filaments of *Phormidium* that are commonly associated with *Fischerella* (U-laminae), and (iii) mucus, diatoms and pyrite framboids (M-laminae). P-laminae dominate most of the columns, with tripartite cycles of P-, U-, to M-laminae being found mostly in the upper parts of the stromatolites. The transition from the P- to U-laminae is marked by a change in the growth pattern of the *Phormidium* and branching of *Fischerella*, which was probably triggered by a change in environmental conditions. In the Frying Pan Lake outflow channel, this change may be related to fluctuations in water level and flow rates that are caused by periods of heavy rain, seasonal changes, long-term variations in rainfall, and/or the unique 40-day hydrological cycle that exists between Frying Pan Lake and Inferno Crater, which is a nearby hydrothermal crater lake.

Keywords Hot spring, lamination, microbialite, siliceous sinter, stromatolite.

INTRODUCTION

Stromatolites, which are laminated microbialites constructed by various microbes (Riding, 1991), are common in hot-spring systems in the geothermal areas of Yellowstone National Park (e.g. Walter *et al.*, 1972, 1976; Walter, 1972; Guidry & Chafetz, 2003a), Iceland (e.g. Konhauser *et al.*, 2001), and New Zealand (e.g. Jones *et al.*, 1997, 1998, 2000). Many stromatolites found in the geothermal systems of the Taupo Volcanic Zone (TVZ) on the North Island of New Zealand have been termed microstromatolites because of their small size (Jones *et al.*, 1997, 2000). Indeed, with the exception of the stromatolites found around the edge of Ohaaki Pool (Hunt, 1997; Jones *et al.*, 1998, figs 2A and 3), large stromatolites are rare in New Zealand hot-spring systems. Stromatolites growing around Frying Pan Lake, which is located in the Waimangu Thermal Valley (Fig. 1), are important exceptions because of their size (up to 3 m long and 1·5 m wide at water surface) and 'lilypad' morphology (Fig. 2).

The microbial mats responsible for the construction of the stromatolites at Frying Pan Lake, in warm (48–52 °C), acidic (pH: 5·6–5·8), spring-fed waters, are dominated by *Phormidium*. These lilypad stromatolites are significantly different

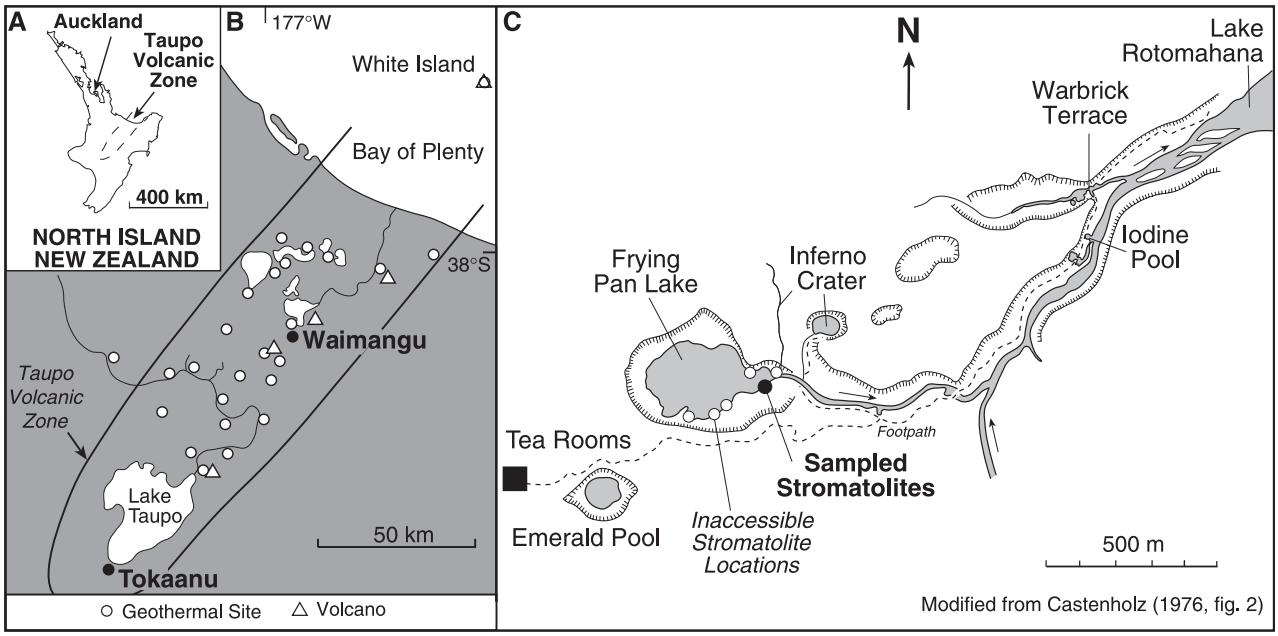

Fig. 1. Location of stromatolites. (A) Map of North Island, New Zealand, showing location of Taupo Volcanic Zone. (B) Location of Waimangu Volcanic Valley. (C) Location of stromatolites. Map modified from Castenholz (1976, fig. 2).

from stromatolites formed by *Phormidium*-dominated microbial mats elsewhere, which commonly have a coniform morphology (e.g. Walter *et al.*, 1976; Love *et al.*, 1983; Walter, 1983; Jones *et al.*, 2002). In this paper, the morphology of the Frying Pan Lake stromatolites and the microbes that mediated their formation are described, and then the silicification and preservation style of those microbes are assessed. This information is used to analyse the growth dynamics of the microbes in terms of their environmental setting and allows comparison with coniform stromatolites that are also constructed by *Phormidium*-dominated microbial mats. The results of this study have broad implications for understanding the growth and preservation of stromatolites of all ages.

MATERIAL AND METHODS

The Waimangu geothermal area, including Frying Pan Lake, is a protected site governed by the Department of Conservation, New Zealand. Therefore, sampling was conducted to minimize impact to the site. In February 2003 and March 2004, detailed observations were made in the field, *in situ* water temperature and pH measurements were obtained, water samples were collected for analysis, and samples from the stromatolites were collected. Only those stromatolites located along the southern shore of Frying Pan Lake near the outflow channel (Figs 1C and 2A) could be studied because of the hazardous, soft ground around much of the shoreline. Samples of the stromatolites were kept in airtight

Fig. 2. Field photographs of stromatolites in Frying Pan Lake outflow channel (see Fig. 1C for location). (A) General view showing stromatolites (white arrows) located along south shore and north-east corner of outflow channel; S = subaqueous springs. Black arrow indicates flow direction. Photograph taken in February 2003. (B) Shallow water along south shoreline of outflow channel with green microbial mat on channel floor, isolated columns that do not reach water level (white arrows), two large lilypad stromatolites, and loose floating pieces of microbial mat along the shore. Largest lilypad stromatolite is *ca* 0·75 m in diameter. Photograph taken in March 2004. (C) Columns that do not reach water level. Note gas bubbles in water. Photograph taken in March 2004. (D) Lilypad stromatolite with outer, dark green raised rim surrounding flat interior that is covered by orange and light green microbial mats. Interior part of lilypad is covered by water that is up to 5 mm deep. Note gas blisters in light green mat and gas bubbles in surrounding water. White arrow indicates flow direction. Photograph taken in March 2004. (E) Lilypad-shaped stromatolite showing orange mats in centre, dark green mat around raised edge, scattered patches of uncovered opal-A (white), and small pieces of desiccated microbial mats resting on stromatolite surface. Photograph taken in February 2003.

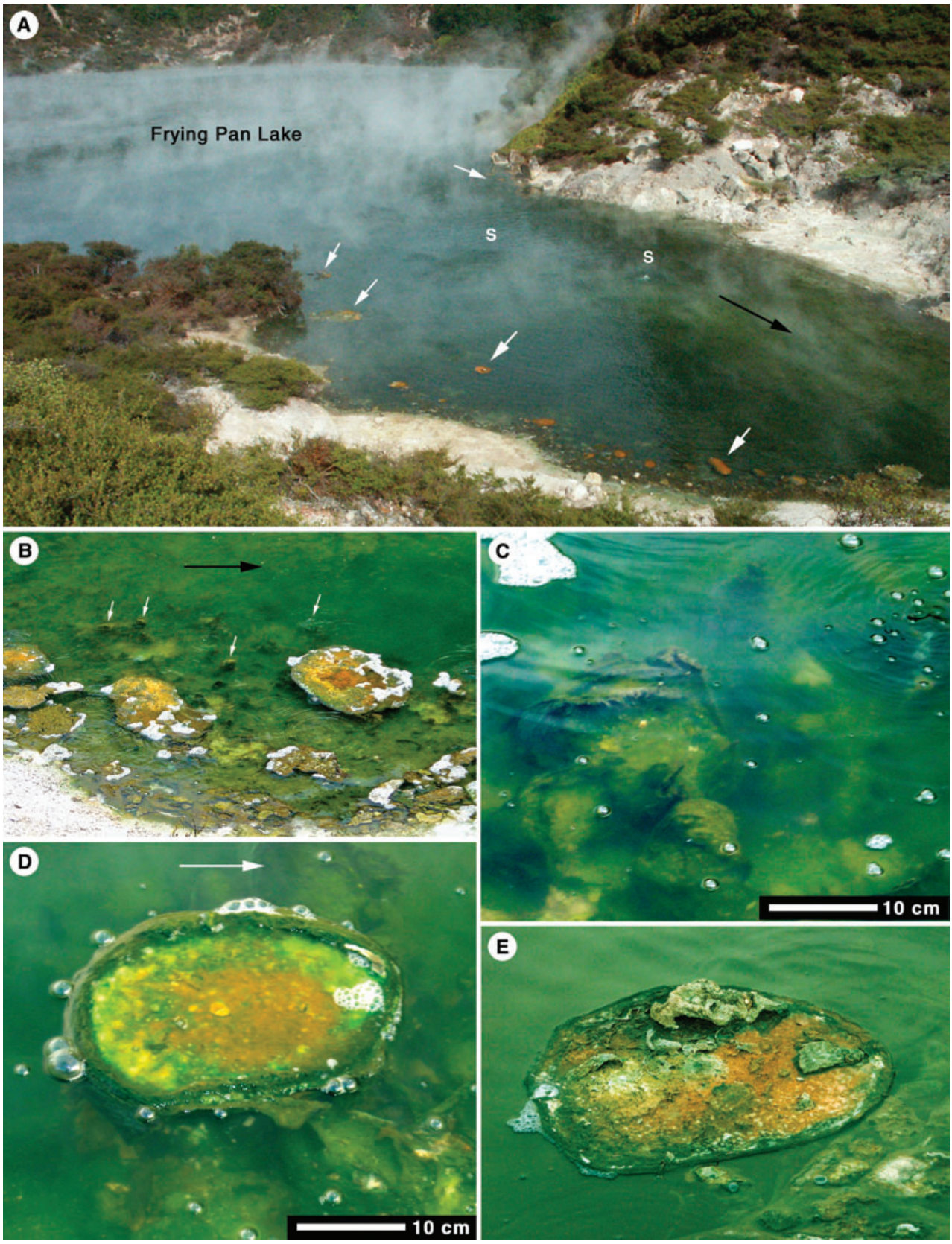
A
Frying Pan Lake
S
S
B
C
10 cm
D
10 cm
E

polyethylene containers and plastic bags until they were air-dried prior to having thin sections made and samples prepared for examination on the scanning electron microscope (SEM).

The stromatolites are poorly lithified despite silicification of the constituent microbes. Thin sections could be made only from epoxy-impregnated samples. Small fractured samples were mounted on SEM stubs and coated with a very thin layer of gold before being examined on a JEOL 6301FE field emission SEM (JEOL USA Inc., Peabody, MA, USA) at an accelerating voltage of 2·5–5·0 kV. The high microporosity and poor lithification of these samples, however, caused considerable charging that made acquisition of high-quality images difficult. This problem was overcome by embedding the most lithified parts of the samples in a highly conductive glue and examining them on the SEM immediately after they had been sputter-coated with gold. The size and morphological features of the constituent microbes were determined from the SEM photomicrographs.

Samples of the actively growing mats were also examined on a transmission electron microscope (TEM). Such samples were stored in 3% glutaraldehyde before being washed three times in phosphate-buffered saline (PBS) with the samples remaining in the buffer for 10 min between each wash. Samples were then stained with 2% osmic acid for 2 h, after which they were washed with PBS repeatedly. Serial dehydration was performed using ethanol concentrations increasing in 10% increments, from 20% to 100%, with a 15 min incubation at each increment. Samples were further incubated in 1 : 1 propylene oxide : 100% ethanol, followed by propylene oxide, for 15 min each, after which they were left in 1 : 1 propylene oxide : spurr resin for 12 h. Samples were embedded in spurr resin and cured in a vacuum oven at 60 °C for 24 h, after which they were sectioned using a Reichert-Jung ultracut microtome, collected on copper grids and examined with a Morgani 268 Philips TEM (FEI Electron Optics, Eindhoven, the Netherlands). Some grids were subsequently stained with 1% uranyl acetate to enhance the contrast of the cell material.

GEOLOGICAL SETTING

The Waimangu-Rotomahana hydrothermal system lies along the southern margin of the Okataina Volcanic Centre in a rugged terrain of Quaternary rhyolitic strata and hydrothermal explosion breccias (Seward & Sheppard, 1986). This region has had a long history of intense volcanic activity including the 1886 eruption of Mt Tarawera, which initiated the present geothermal system. Frying Pan Lake, the focus of this study, occupies part of Echo Crater, which formed during the 1886 Tarawera eruption. The present lake was formed after a major hydrothermal eruption on 1 April 1917, after which time water from thermal springs and runoff gradually filled the enlarged depression (Keam, 1955; Houghton & Scott, 2002).

Frying Pan Lake, which has a surface area of *ca* 38,000 m^3 (Scott, 1994), is bounded by steep and nearly vertical walls composed largely of rhyolitic ashes overlain by mud and explosion breccias. The lake floor is flat, averaging *ca* 6 m deep, but is locally > 20 m deep where hot springs and gases are discharged from vents in the sediments of the lake floor (Keam, 1981; Houghton & Scott, 2002). Frying Pan Lake has been described as the world's largest hot spring, but the multiple vents and the contribution of catchment waters make the term 'hydrothermal lake' more appropriate.

The lake waters are of acid sulphate type with a pH range of 5·4–5·8 (Glover *et al.*, 1994, their table 2). The waters are derived from deep alkaline chloride waters that have been acidified by the atmospheric oxidation of H_2S gas, which has increased their sulphate concentration above that of most other fluids at Waimangu (Mahon, 1965; Hunt *et al.*, 1994). Small, dilute acid sulphate springs (pH 2·5) with very low chloride concentration discharge into the lake around the shoreline, together with a few alkaline chloride springs less modified by H_2S oxidation. Silica concentrations are 335–428 mg l^{-1} (Table 1). Water temperatures in the lake have consistently ranged between 45 and 55 °C for several decades.

The lake surface is continuously disturbed by rising convectional plumes of water and gas that break at the surface, generating concentric surface waves above each plume, interference waves where adjacent plume waves interact, and general turbulence. These surface waves, in turn, are active in the littoral zones where the stromatolites are growing, even at times when wind-generated wave activity is low.

The lake waters flow eastwards into Hot Water Creek, which is supplemented by many alkaline hot springs, before it drains into Lake Rotomahana. The water depth at the outlet is 0·5–1·5 m. Discharge from the lake, which is 65–220 l sec^{-1} and averages *ca* 110 l sec^{-1} (Scott, 1994; Houghton

Table 1. Water analyses for Frying Pan Lake, associated springs, and outflow channel from Frying Pan Lake.

Reference	Date	*T* (°C)	pH	Li	Na	K	Mg	Ca	SiO_2	B	F	Cl	SO_4	HCO_3
Grange (1937) – 28[1]	April 1928	55–59	3·0		607	70	4	17	428	14·0		953	262	
Grange (1937) – 29[1]	June 1932	55–59	3·1		609	51	4	14	412	4·0		878	262	
Sheppard (1986) – UO1[2]	April 1982	95	2·2	0·12	56	19	7·53	37	312	0·2	0·12	5	1345	
Sheppard (1986) – UO1[2]			6·2	2·90	500	55	1·08	7	381		3·2	680	270	34
Sheppard (1986) – UO2[2]	April 1982	91	8·0	1·90	345	37	5·15	10	344	3·3	1·3	434	120	204
Sheppard (1986) – UO2[2]			7·7	1·70	340	46	5·8	10·7	335	5·0	1·1	425	126	145
Sheppard (1986) – UO3[2]	April 1982	52	4·3	3·20	495	45	1·8	6·2	351	5·9		708		
Weissberg (1969, Table 2)[3]		67	3·8	3·20	545	49			380			762	320	
Mann *et al.* (1986)[4]	1980s	54	3·5		497	45	1·66	7·1	389	6·2		700	247	37
Seward & Sheppard (1986)[5]	1982	52	4·5		514	45	1·7	4·3	389	7·0		674	242	nd
This study[6]	February 2003	47–51	5·8	2·10	502	41	1·84	5·6	374	6·8	0·4	682	233	

Units expressed in mg kg^{-1} except those of Grange (1937), which are given in p.p.m.
[1]From Grange (1937) when Frying Pan Lake consisted of smaller spring-fed lakes on Frying Pan Flat.
[2]From Sheppard (1986): UO1 – bubbling springs on margin of Frying Pan Lake; UO2 – geyser on the eastern lake shore; UO3 – outflow channel near stromatolites examined in this study.
[3]From Weissberg (1969, table 2), values from Mahon (1965).
[4]From Mann *et al.* (1986).
[5]From Seward & Sheppard (1986).
[6]This study, around stromatolites in outflow channel from Frying Pan Lake.

& Scott, 2002), is controlled by hydrodynamic and climatic variables. Minor discharge fluctuations of 1–3 days duration have been attributed to rainfall-induced runoff in the catchment (Scott, 1994), with some cool meteoric groundwater discharge around the lake margins. A decrease in discharge from 122 to 104 l sec^{-1} between 1972 and 1990 was related to a decrease in rainfall during that period (Scott, 1992, 1994).

Superimposed on these climatic fluctuations is a cyclic variation in water level that is related to the unique hydrothermal relationship between Frying Pan Lake and Inferno Crater Lake (Lloyd, 1973, 1974; Scott, 1992, 1994; Glover *et al.*, 1994). Inferno Crater (Fig. 1C), located 300 m to the NE, follows a 40-day cycle with the water surface in the crater rising slowly until it reaches a level where it flows through a outflow channel into Hot Water Creek for a few days (Seward & Sheppard, 1986; Scott, 1992, fig. 3; 1994; Glover *et al.*, 1994). The water level in the crater then drops to its lowstand position and the cycle begins again. Water discharge from Frying Pan Lake decreases while the water is flowing out of Inferno Crater Lake (Lloyd, 1973, 1974; Seward & Sheppard, 1986; Scott, 1992, 1994; Glover *et al.*, 1994). Then, while the water level in Inferno Crater Lake falls, the outflow from Frying Pan Lake increases. These cyclic changes account for the *ca* 20 l sec^{-1} difference in the flow rate from Frying Pan Lake, but only minor changes (few centimetres) in water level.

Historical records show that the water in the outflow channel from Frying Pan Lake has had a temperature (*T*) of 51–67 °C and a pH of 3–8 (Table 1). Much of that variation can be related to local input from sub-aqueous springs, sub-aerial springs along the shoreline, and streams that flow into the lake (Brock & Brock, 1971). In February 2003 and March 2004, surface water around the stromatolites on the south side of the outflow channel (Fig. 2A) had a temperature of 47–51 °C and a pH of 5·5–5·8 (Table 1).

Mastigocladus laminosus, *Phormidium* sp., and *Cyanidium caldarium* were found by Brock & Brock (1970, 1971) in the environs of Frying Pan Lake and its outflow channel. Much of their material came from Trinity Terrace, which was located on the south-central shore of Frying Pan Lake before it was destroyed by a hydrothermal eruption on 22 February 1973 (Lloyd & Keam, 1974; Scott, 1992). Brock & Brock (1970) argued that the distribution of these taxa was controlled by the balance between water temperature and water acidity. The central parts of the outflow channel appear free of visible cyanobacterial mats because the temperature is >56 °C. Microbes thrive in the marginal zones where the water is a little cooler (51–55 °C). *Cyanidium caldarium*, an obligate acidophile, was found where the pH < 4·8, whereas *Mastigocladus* (now known as *Fischerella*) and *Phormidium* were found where the pH > 4·8 (Brock & Brock, 1970, 1971).

Seward & Sheppard (1986, their plates 7.3 and 7.4) illustrated siliceous stromatolites growing in the outflow channel from Frying Pan Lake that contained ferruginous precipitates with a high

content of tungsten. Tungsten-rich stromatolites were not found during the course of this study.

STROMATOLITES

The lilypad stromatolites were found to be growing at several locations around the shoreline of Frying Pan Lake and along its outflow channel up to 200 m downstream from the outlet (Fig. 1C). The stromatolites form discrete columns that are rooted on shallow (< 1 m) platforms around the lake margins or form ledges that extend from the shoreline or channel margins (Fig. 2A,B,D,E). The largest stromatolites, which are inaccessible, are estimated to be up to 3 m long, 1·5 m wide, and 0·5–1 m high. The stromatolites examined were sampled along the southern shoreline of the outflow channel, 10–50 m east of the outlet (Figs 1C and 2A). Lilypad stromatolites are most common within 2 m of the south shoreline. Several submerged columns that have not yet reached the water surface are present in the deeper parts of the channel, but only a few offshore examples have developed the full lilypad morphology. Several lilypad stromatolites are present on the northern shore of the channel near its junction of the lake and *ca* 50–100 m downstream (Fig. 2A). The stromatolites grow in water that is 15–50 cm deep where sampled.

The floor of the proximal outflow channel, which is *ca* 1 m deep, is covered with a dark green microbial mat (Fig. 2B–D). Columns of various shapes and sizes grow to various heights above the channel floor (Fig. 2B,C), both along the margins and in the axial parts of the channel. These columns are formed of dark green microbial mats that appear to be identical to those that coat the surrounding substrate. Some columns show continuity with the benthic mats around the base of the columns. Most of the blade-shaped and ovate columns, which are formed entirely of the microbial mat, flex with local current and wave motion. The larger columns commonly have a dense and rigid core that appears to be formed of silicified microbial mats or small boulders. In some cases, strands of filamentous microbes extend from the tops of the submerged columns and are aligned parallel to the prevailing local currents. Once the top of a column has grown upwards to reach the water level, the mats then extend outwards at water level to produce the round to ovate lilypads (Fig. 2). In cross-section, these stromatolites are mushroom-shaped because outward growth at their tabular upper surface far exceeds the expansion of the submerged column (Fig. 3). Lateral expansion is greatest on the downstream side of many stromatolites with overhangs of up to 10 cm being evident on some stromatolites. Such overhangs shade the parent column from direct sunlight (Fig. 3). The overhangs are formed of densely interwoven, flexible microbial mats that have undergone relatively little silicification. As a result, the overhangs can flex in response to changes in water level or currents.

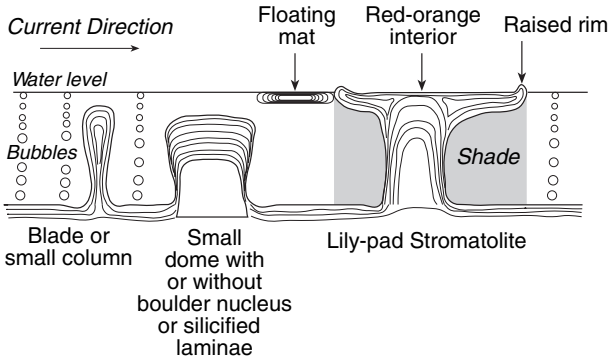

Fig. 3. Schematic diagram showing development of microbial mat into blades, small columns, small domes, and lilypad stromatolites. Floating mat is derived from disruption and breakage of mat on channel floor. Overhangs developed on lilypad stromatolites shade the central columns and mat on channel floor from sun. The extent of shaded area depends on angle of the sun relative to lilypad stromatolite.

The upper surfaces of the lilypad stromatolites are distinctive because of the vivid colours of the microbial mats, which seem to vary in accordance with the amount of water present on their surfaces (Fig. 2). The raised (3–5 mm high) rims, which maintain contact with the surrounding water, are dark green (Fig. 2D). When wet, the mats that cover the flat interior of the lilypad surface have an orange-red interior zone that is surrounded by a light green zone (Fig. 2D). After extensive drying, the light green zone commonly becomes orange-red and the interior zonation is lost (Fig. 2E). Slightly higher water levels lead to flooding of lilypad interior with the depth being controlled by the height of the raised rim. When water levels are low, the interior of the lilypad becomes exposed and partial drying of the microbial mats commences. As that water level drops, gas bubbles rise through the mat and create small blisters in the exposed microbial mat (Fig. 2D). Some of the lilypad stromatolites have white partly silicified mats in their central parts (Fig. 2E).

The mats that cover the channel floor are commonly fragmented by gas bubbles and spring waters that are continually escaping from some of the submerged vents. These mat fragments become buoyant, possibly because of trapped gases, and float to the water surface where they move in accordance with local current and wind directions. Storms and high rainfall events, such as that in December 2004, can also lead to the mats being torn up and fragmented. The mat fragments are periodically blown onto the southern shoreline, forming brush-heaps of mat detritus. Some broken mats get lodged between the lilypad stromatolites that grow in that area (Fig. 2A). Further lateral growth of the fragmented mats locally produces an interlocking semi-continuous mat along the littoral zone. Mats that have accumulated along the shoreline become partially silicified by wicking of spring waters and capillary evaporation. Some of the mat fragments become partly silicified while floating on the surface of the water, whereas others are washed onto the surface of the lilypad stromatolites (Fig. 2E).

The mats on the upper surface of the stromatolites are formed almost entirely of non-branching, septate filamentous microbes, *ca* 1·5 μm in diameter, that have their trichome enclosed in a thin (< 0·2 μm) sheath (Fig. 4A,B). The presence of intracellular photosynthetic membranes (Fig. 4B) clearly confirms their photosynthetic nature. This, coupled with their general morphology, suggests that they are probably *Phormidium*.

In TEM thin section, it is readily apparent that the sites for opal-A nucleation are on the sheath surface, a feature previously noted in other cyanobacteria (e.g. Phoenix *et al.*, 2000; Konhauser *et al.*, 2001). Individual opal-A spheres are *ca* 100 nm in diameter, but in some areas on the cell surface they have merged into a thick, dense silica coating. The presence of what appears to be an intact cytoplasm in some of the mineralized cells (Fig. 4C), suggests that silicification began while the cell was still viable.

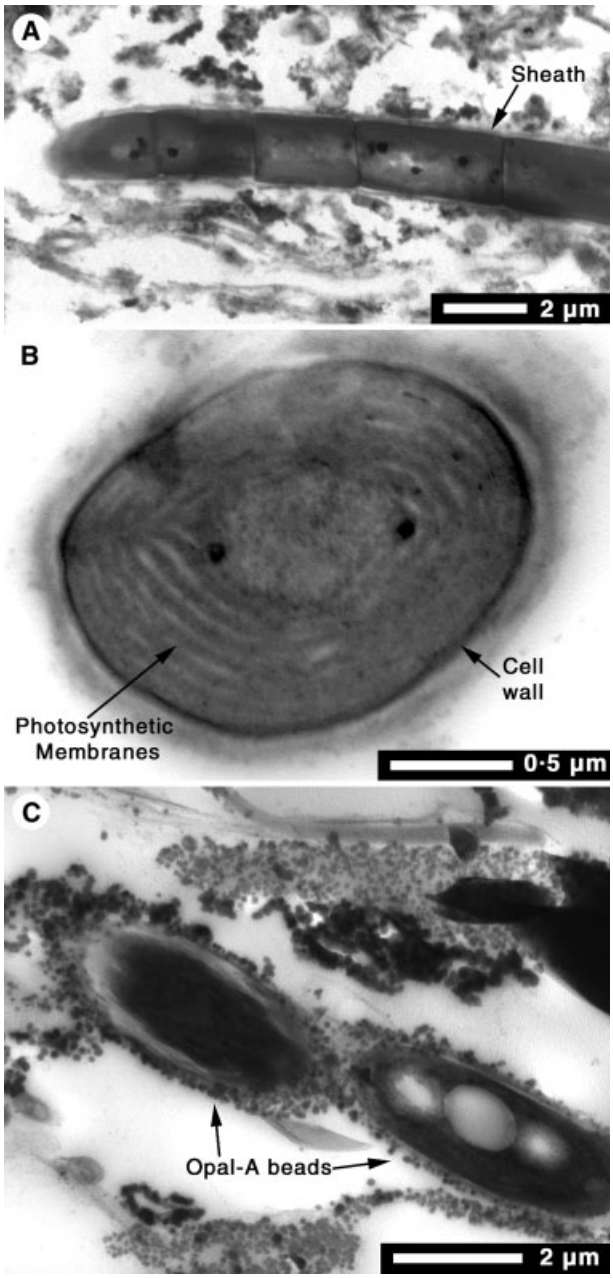

Fig. 4. TEM images of *Phormidium* from mat on surface of stromatolite. (A) Longitudinal section through filament showing cells and thin sheath. (B) Transverse cross-section through filament showing photosynthetic membranes (PM) and cell wall (CW). (C) Longitudinal section through filament showing external epicellular silicification and intact cytoplasm.

Silicified biota

Phormidium and locally, *Fischerella* dominate the silicified microbiota in the stromatolites (Figs 5–11). Minor components include indeterminate septate filamentous microbes, small-diameter filamentous microbes, perforate and non-perforate spores (Fig. 12), and diatoms (Fig. 13).

Phormidium

Castenholz *et al.* (2001) included *Phormidium* in the form genus *Leptolyngbya* Anagnostidis & Komarek 1988 that includes a large number of filamentous cyanobacteria from hypersaline, saline and freshwater habitats, including hot springs with temperatures up to 63 °C. These microbes

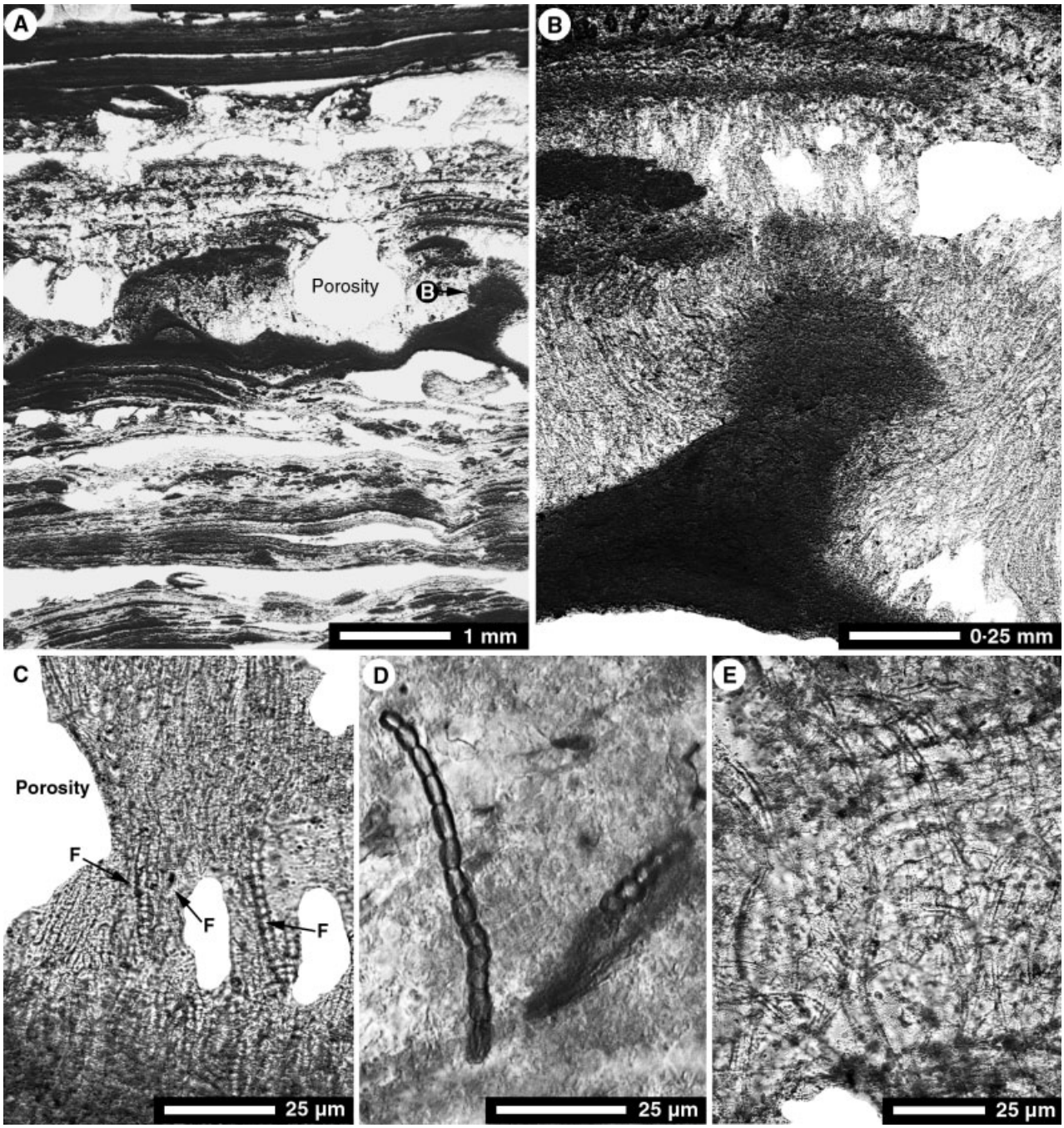

Fig. 5. Thin-section photomicrographs of stromatolites from outflow channel from Frying Pan Lake. Entire stromatolite formed of opal-A. (A) Vertical cross-section through upper part of stromatolite showing laminae formed of small filamentous tufts sandwiched between flat- to wavy laminae. Note high porosity (white). (B) Enlarged view of filamentous tuft shown in (A) (position indicated by white letter B). Column formed of dense array of heavily silicified filamentous microbes surrounded by filamentous microbes that are not as heavily silicified. (C) Basal part of filamentous tuft formed of *Fischerella* (F) intermixed with *Phormidium*. (D) *Fischerella* embedded in opal-A matrix. Note well-defined cells that vary in size within one filament and between filaments. (E) Tangled mat of *Phormidium* in upper part of filamentous tuft.

have narrow (< 3 µm diameter) trichomes. Sheaths characterize many taxa in this group. In general, this form genus is equivalent to the *Lyngbya* Agardh 1824–*Phormidium* Kützing 1843–*Plectonema* Thuret 1875 group (LPP) as defined by Rippka *et al.* (1979). The inclusion of all of these genera in one form genus reflects the taxonomic uncertainty that surrounds this group

of cyanobacteria. As a result, many genera included in the LPP group or the form genus *Leptolyngbya* are still referred to by their traditional names (Hindák, 2001).

Phormidium is an architecturally simple, non-branching filamentous cyanobacterium that has a trichome encased by a thin, gelatinous sheath (Copeland, 1936; Nash, 1938; Cassie, 1989). Numerous extant species have been named according to their filament diameter (Copeland, 1936; Nash, 1938; Cassie, 1989), the presence or absence of granules on their cross-walls (Nash, 1938), their habitat (Nash, 1938), the apex morphology of the trichome, and/or cell size (Copeland, 1936). Most of these features are not evident in silicified specimens and it is therefore difficult to ally silicified forms to extant taxa (Jones *et al.*, 2002).

The microbiota in the stromatolites from Frying Pan Lake is dominated by non-branching filamentous microbes (Figs 5–8) that have an external diameter of 1·6–3·1 μm (Fig. 9A) and a lumen diameter of 0·6–0·9 μm (Fig. 9B). The external diameter is primarily a reflection of the thickness of opal-A that was precipitated around the silicified filament. Transverse cross-sections through some specimens reveal a discontinuity (Jones *et al.*, 2001) that separates the silicified sheath from the opal-A that was precipitated around the sheath as a cement (Fig. 7E–I). The lumen diameter, which can generally be equated to the diameter of the original trichome, providing there is no evidence of opal-A precipitation in the open lumen (Merz, 1992), is 0·6–0·9 μm, with a distinct mode between 0·7 and 0·8 μm (Fig. 9B). This is consistent with many extant species of *Phormidium* (see Jones *et al.*, 2002, fig. 17).

Fischerella

Mastigocladus, and *Hapalosiphon* are treated here as synonyms of *Fischerella* Gomont 1895 because Hoffmann & Castenholz (2001) have suggested that there is not sufficient reason to consider them separate genera. *Fischerella*, a monospecific genus characterized by significant morphological variation (Castenholz, 1978), generally grows in waters with a temperature of 28–64 °C and a pH of 6·8–9·0 (Copeland, 1936; Castenholz, 1969, 1973, 1976; Cassie, 1989). It has, however, been reported from waters with a pH as low as 3·8 (Castenholz, 1973). *Fischerella laminosus* (Cohn 1862) has been found in the hot-spring systems of New Zealand (Castenholz, 1973, 1976; Cassie, 1989), Iceland (Castenholz, 1973; Joergensen & Nelson, 1988; Konhauser *et al.*, 2001), North America (Copeland, 1936), Central America, Japan and Italy (Castenholz, 1973). There are two forms of *F. laminosus*: the mid-temperature form (MTF) that has an upper temperature limit of 57 °C, and the high-temperature form (HTF) that has an upper temperature limit of 63–64 °C (Castenholz, 1969, 1973, 1976, 1978). The MTF is characterized by true and inverted V-branching whereas the HTF is unbranched (Castenholz, 1973). Incipient V-branching is found, however, in some of the lower temperature variants of the HTF (Castenholz, 1973). *Fischerella* is a resilient microbe that can withstand extremes of dryness and freezing (Castenholz, 1973).

Some laminae in the stromatolites from Frying Pan Lake contain scattered filaments of *Fischerella* or small tufts formed of *Fischerella* intertwined with *Phormidium* (Figs 5B,C and 10). The trichomes are formed of short cylindrical (Fig. 10C) to barrel-shaped (Fig. 10D,E) cells that are 2·5–9·7 μm (average 5·1 μm) long, 3·0–5·2 μm (average 4·2 μm) wide, and have a width/length ratio of 0·4–1·7 (average 0·9) (Fig. 11). Cellular dimensions are highly variable in individual trichomes (Figs 5D and 10B) and between trichomes (Fig. 10B), even between neighbouring trichomes from the same tuft. There is an exponential decrease in the cell width/cell length ratio relative to cell length (Fig. 11B). The septa between successive cells are pierced by a pore channel (Fig. 10C–G) that house the 'pit connection' that joined adjacent cells. The thin, silicified cell wall is formed of numerous small rounded to ovate opal-A platelets (Fig. 10F,H). Uniseriate primary trichomes lie parallel to the depositional surface (Fig. 10I,J). Secondary trichomes, which originate by branching from the primary trichomes, arise from cells that are either sub-spherical or have their long axis (sub-)perpendicular to the depositional surface (Fig. 10I–K). One (Fig. 10J) or two (Fig. 10L) branches may arise from a single cell in the primary trichome. The presence of branching fingerprints the microbe as MTF as defined by Castenholz (1969, 1973, 1976, 1978). This is consistent with the water temperature of 47–51 °C where the stromatolites grow.

Other microbes

Microbes other than *Phormidium* and *Fischerella* form < 5% of the biota in the stromatolites (Fig. 12). Their scarcity means that it is difficult to establish all of their morphological attributes and hence, identify them in terms of extant taxa without the use of DNA fingerprinting.

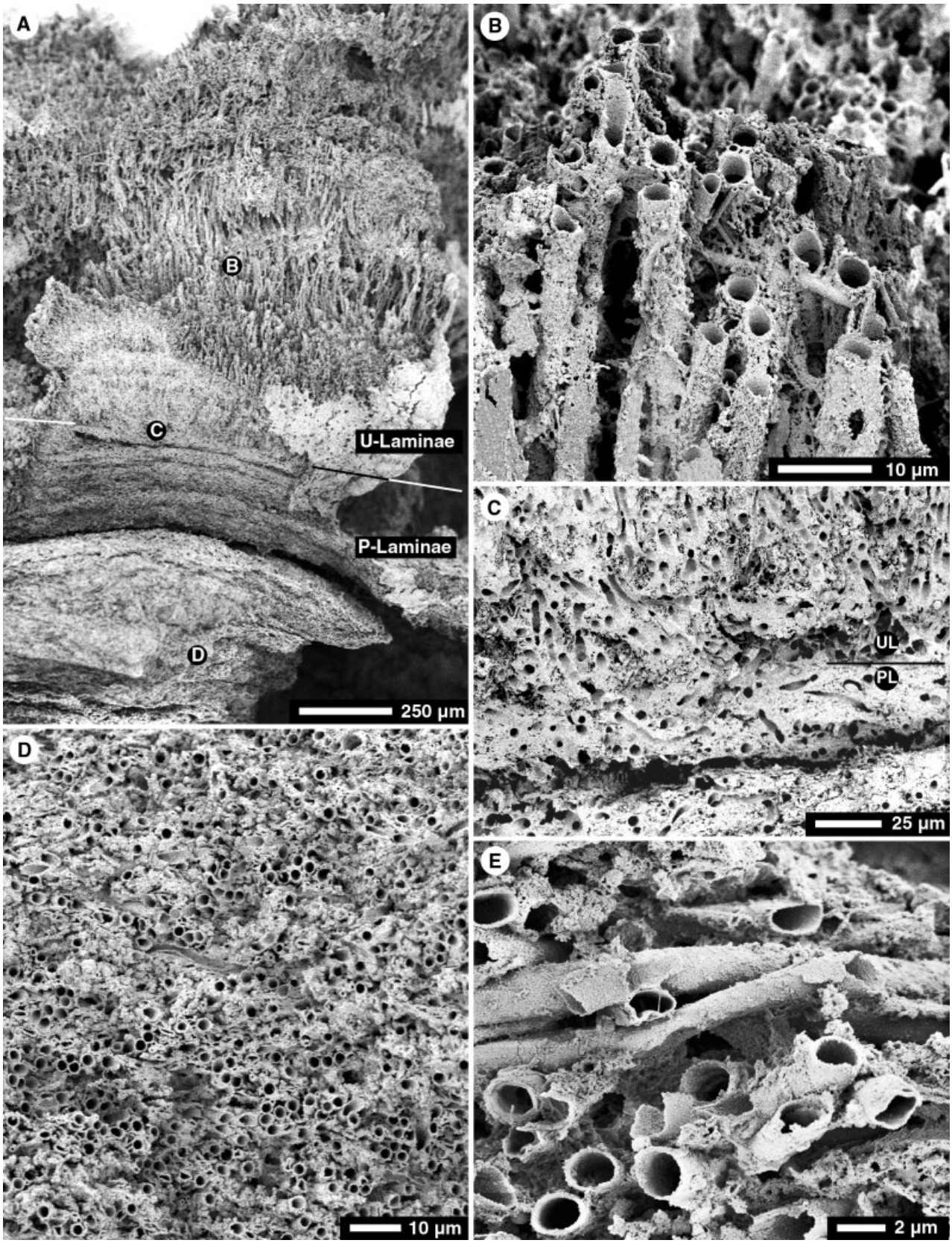
A
B
C
U-Laminae
P-Laminae
D
250 µm
B
10 µm
C
UL
PL
25 µm
D
10 µm
E
2 µm

Internal structures

The stromatolites from Frying Pan Lake are formed of: (i) 'P-laminae' that are characterized by prone filamentous microbes, (ii) 'U-laminae' that are characterized by upright filamentous microbes, and (iii) 'M-laminae' that are characterized by extracellular mucus, pyrite framboids and diatoms.

P-laminae

The P-laminae are formed almost entirely of densely interwoven, flat-lying filaments of *Phormidium* (Figs 6D,E and 7), with only scattered specimens of other microbes. In any given lamina or succession of P-laminae, the *Phormidium* filaments tend to lie parallel to each other (Fig. 6D). The orientation of filaments in successive layers, however, commonly varies by as much as 90° (Fig. 6E). The deformed cross-sectional shape of many filaments indicates that many were partly crushed before they were silicified (Fig. 7D,G). The P-laminae have a high microporosity because most lumens and interfilament spaces are open (Figs 6D,E and 7A–D). Locally, however, porosity is reduced by isopachous layers of opal-A cement that coat the filaments (Fig. 7G–I).

U-laminae

The U-laminae have a more diverse biota than the P-laminae. Although *Phormidium* dominates these laminae, *Fischerella* are locally common (Figs 5C,D and 10) and other unidentified microbes (Fig. 12) are scattered throughout. The *Phormidium* filaments were not deformed prior to silicification (Fig. 8B,D,E). Compared with the P-laminae, filaments in the U-laminae are less densely packed and have a greater thickness of encrusting opal-A (Figs 8 and 10). Silicified epiphytes are present on many of the silicified filaments of *Phormidium* (Fig. 8C,D). Spaces between the vertical filaments are partly filled with complex networks of silicified filaments (Fig. 8E,F). The taxonomic affinity of the epiphytic microbes and those forming the networks is unknown because of the encrusting opal-A masking their morphological features.

M-laminae

The M-laminae, generally < 100 μm thick, are formed of mucus (exopolymers), pyrite framboids, and scattered diatoms (*Pinnularia*?) (Fig. 13). These laminae, which are far less common that the P- and U-laminae, probably form < 5% (based on visual estimates from SEM samples) of the stromatolites. Pennate diatoms are the only microbes visibly preserved in these layers and it is therefore tempting to suggest that they secreted the mucus. Pyrite framboids, up to 5 μm in diameter, are common in these layers (Fig. 13), but rare to absent in the other types of laminae. Each framboid contains 20–70 microcrystallites (Fig. 13C). In places, the framboids have disintegrated and their constituent subcrystals, up to 1 μm long, are scattered amid the mucus coating (Fig. 13C).

PATTERNS OF MICROBE SILICIFICATION

Studies have shown that microbes will only be preserved if silicification takes place within 10–12 days of their death (Bartley, 1996). Similarly, Jones & Kahle (1986) argued that rapid mineralization must take place if mineralized microbes are to retain their three-dimensional form. Even with such rapid silicification, many of the morphological features critical for identification of the microbes will be lost (Jones *et al.*, 2001, 2004).

The three-dimensional preservation of the microbes in the stromatolites from the outflow channel from Frying Pan Lake (Figs 6–8, 10 and 12) attests to their rapid silicification. The *Fischerella* are very well preserved with many of their taxonomically important characters being clearly evident (Fig. 10C,D). In contrast, the silicified specimens of *Phormidium* commonly have a distorted cross-section (Figs 6E and 7D,G) and scant other morphological features (Figs 6–8). The distortion of the filaments (Fig. 6G) can probably be attributed to compression between neighbouring filaments that took place before silicification had made them rigid and resistant to distortion. Nevertheless, silicification must

Fig. 6. SEM photomicrographs showing general features of stromatolite from outflow channel from Frying Pan Lake. (A) General view of sample showing P-laminae formed of prostrate filaments overlain by U-laminae formed of erect filaments. White letters B, C, and D indicate locations of (B), (C), and (D). (B) U-laminae formed of upright *Phormidium* encased by silica precipitates and epiphytic microbes. (C) Transition from P- to U-laminae. (D) P-laminae dominated by filaments of *Phormidium* that lie parallel to depositional surface. (E) Enlarged view of P-laminae showing interwoven filaments of *Phormidium*.

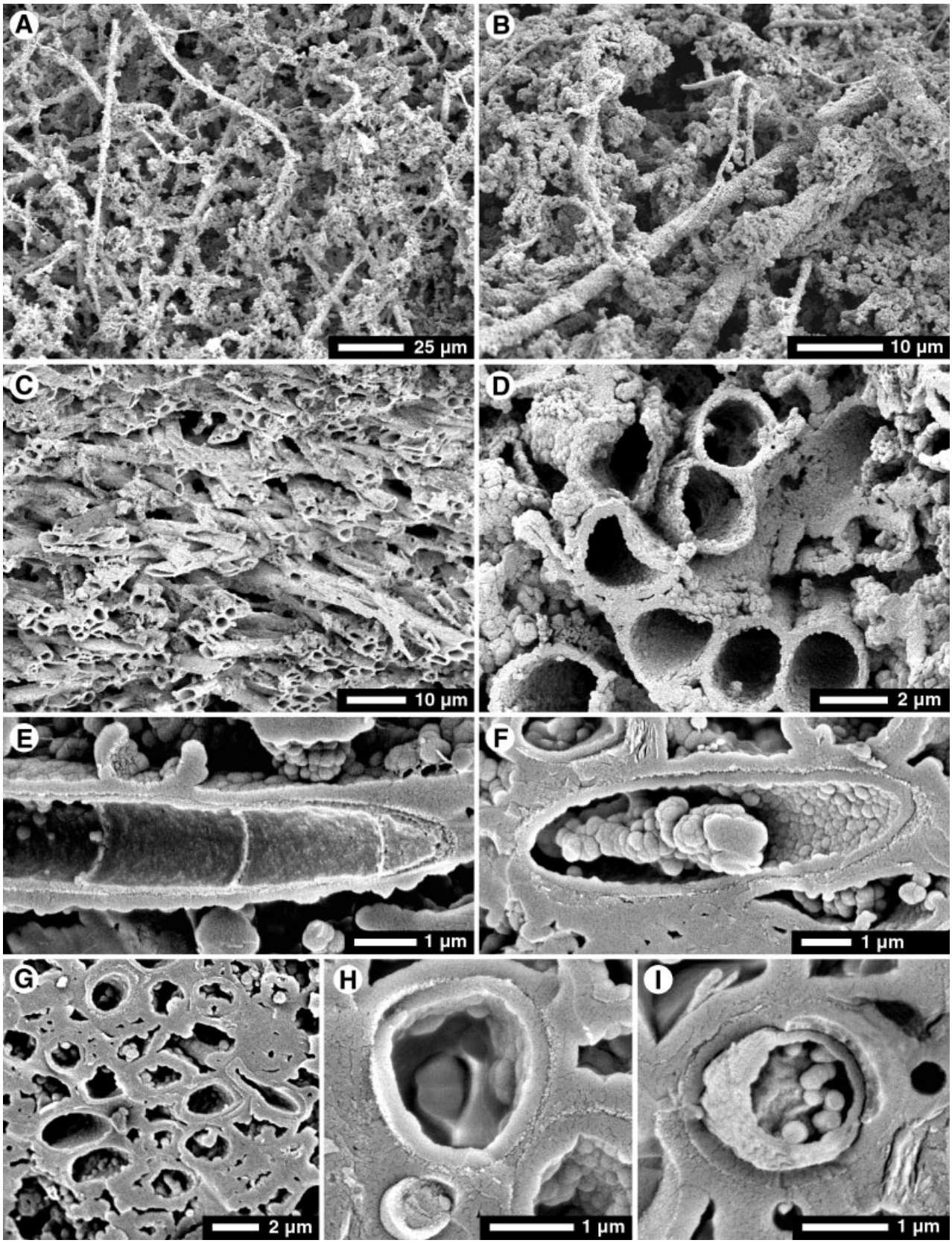
A
25 μm
B
10 μm
C
10 μm
D
2 μm
E
1 μm
F
1 μm
G
2 μm
H
1 μm
I
1 μm

have taken place before the filaments underwent any significant degree of decay.

Some of the silicified filaments were encased by opal-A cement (Fig. 7E–I). In many specimens, there is a distinct discontinuity between the opal-A that replaced the filament and the opal-A that formed as a cement (Jones *et al.*, 2001, fig. 8A–C). Such cross-sections also show that the distribution of the isopachous opal-A cement is highly variable (Fig. 7G,H). Thus, some areas appear to be devoid of such cement (e.g. Fig. 7D) whereas other areas have filaments encrusted with cement (Fig. 7F–I). The isopachous cement layers are < 1 μm thick and there are only scattered examples where the spaces between neighbouring filaments have been completely filled with cement. There is no readily apparent pattern to the distribution of the opal-A cement.

SIGNIFICANCE OF LAMINATIONS IN STROMATOLITES

Stromatolites in the outflow channel from Frying Pan Lake are formed largely of P-laminae (Fig. 5A). P-laminae form most of the central columns that support the lilypad plate. The uppermost parts of the stromatolites are more complex because they are formed of cycles that evolve from P- to U- to M-laminae (Fig. 4A). Individual filaments of *Phormidium* that change from a horizontal to a vertical orientation (Fig. 6C) mark the transition from the P- to U-laminae. Similarly, (sub-)vertical branches of *Fischerella* arise from the uniseriate primary trichome that lies at the top of the P-laminae (Fig. 10A,J–L). The fact that individual filaments of two different taxa change orientation at the same level indicates that a change in environmental conditions may have been responsible. It is difficult, however, to attribute this to a systematic daily or seasonal changes because the stromatolite columns are formed mostly of P-laminae and the tripartite succession of laminae is found only in the upper part of the structures (Fig. 5). This, in turn, suggests that the development of the U- and M-laminae may be related to factors other than time-dependent changes in environmental conditions. These stromatolites grow in flowing water and it seems reasonable to suggest that water level and/or flow directions may influence development of individual laminae in the stromatolites. Thus, even minor changes in flow direction across the surface of the stromatolite might be responsible for the change in the orientation of *Phormidium* in successive layers.

Laminae, which are a definitive element of stromatolites, have been attributed to many different causes. Cyclic alternations of laminae have commonly been ascribed to daily, monthly, annual, or some other time-dependent growth processes (Symoens, 1957; Monty, 1967, 1976; Walter *et al.*, 1972; Park, 1976; Walter, 1976; Golubic & Focke, 1978; Chafetz & Folk, 1984; Chafetz *et al.*, 1991; Freytet & Plet, 1996; Renaut *et al.*, 1996; Jones *et al.*, 1998, 1999; Konhauser *et al.*, 2001; Kano *et al.*, 2003). Nevertheless, it is commonly difficult to determine with any certainty if those cycles represent daily, monthly, annual or some other regular periodic growth (Park, 1976). Caudwell *et al.* (2001), for example, concluded that the laminations in *Rivularia* stromatolites that grew in a palustrine environment in a temperate climate were due to a wide range of biological, environmental and climatic factors that did not necessarily follow a seasonal or annual pattern. Such assessments are especially pertinent in the case of the outflow channel from Frying Pan Lake where the laminae in the stromatolites could potentially be linked to: (i) short-term (1–3 days) increases in outflow caused by heavy rain, (ii) seasonal changes in rainfall and temperature, (iii) changes in outflow related to the 40-day hydrological cycle shared with Inferno Crater Lake, and/or (iv) long-term changes in rainfall between 1972 and 1990 (Scott, 1992,

Fig. 7. SEM photomicrographs of P-laminae in stromatolites from outflow channel from Frying Pan Lake. (A) Depositional surface of P-laminae showing loosely interwoven filaments of *Phormidium*. (B) Enlarged view of depositional surface showing *Phormidium* encased by opal-A precipitates and silicified epiphytes. (C) Vertical cut through P-laminae showing interwoven filaments of *Phormidium*. (D) Enlarged view of prone filaments of *Phormidium* showing thin silicified walls and open lumen. Note that some filaments were partly crushed prior to silicification. (E) Oblique longitudinal section through *Phormidium* showing silicified sheath, location of septa, and opal-A encrustation. (F) Oblique transverse cross-section through *Phormidium* showing silicified sheath, encrusting opal-A, and silicified trichome(?). (G) Vertical cross-section through P-laminae showing prone *Phormidium* with variable cross-section shapes caused by partial crushing of filaments prior to silicification. (H) Transverse cross-section through *Phormidium* showing silicified sheath, open lumen, and encrusting opal-A. (I) Transverse cross-section through *Phormidium* showing silicified sheath encasing a silicified trichome (?).

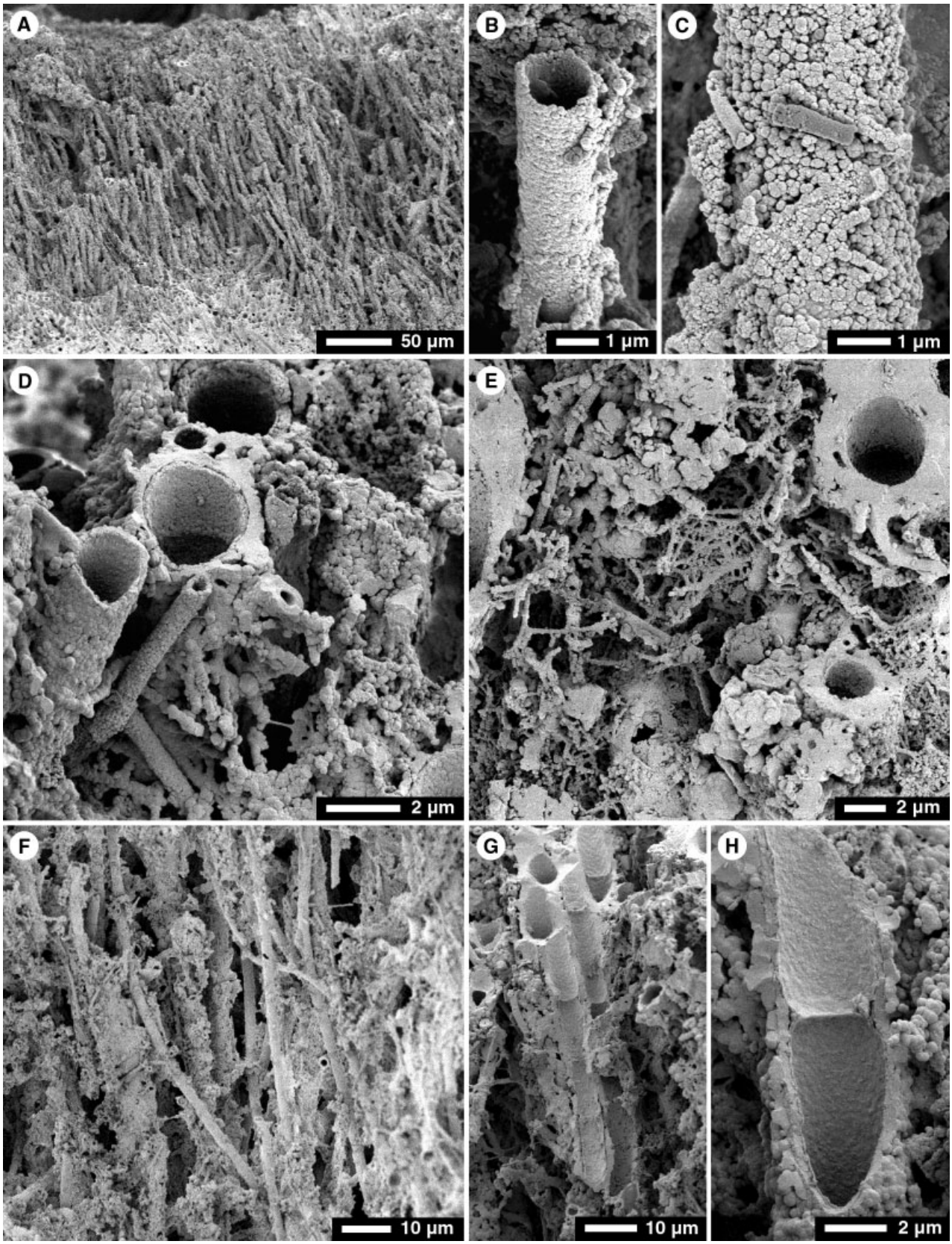
A
50 μm
B
1 μm
C
1 μm
D
2 μm
E
2 μm
F
10 μm
G
10 μm
H
2 μm

1994). It is difficult to correlate the laminae in the Frying Pan Lake stromatolites with any of these variables.

DISCUSSION

The lilypad morphology of the Frying Pan Lake stromatolites is unusual and seemingly quite rare. This form was not recognized in Hofman's (1969) classification of stromatolite morphotypes. Davis (1897, fig. 7) described and illustrated 'pillars' from an unnamed pool in Yellowstone National Park that '…spreads out at the surface of the water in a form that resembles the umbrella-like top of a toadstool.' He could not find any direct evidence that '…siliceous matter was secreted directly around the fibers [filaments], for the deposits were in the form of granules of amorphous silica distributed among the filaments.' Nevertheless, Davis (1897) did suggest that the filamentous microbes were actively involved in the construction of the pillars because the '…presence of the algal filaments as foreign bodies encourages the deposition of silica…'. To our knowledge, this type of stromatolite has not been described or illustrated from anywhere else.

Lilypad structures and ledges, first described from cave pools, are usually composed of $CaCO_3$ precipitated from the pool waters (e.g. White, 1976; Gonzalez & Lohmann, 1988; Hill & Forti, 1997). Ledges and lilypads may unite at the water surface to form a continuous plate of precipitated minerals that will extend outwards until it fractures or sinks under its own weight. Similar morphological forms have since been recognized in modern hot-spring pools (Renaut *et al.*, 1999; Campbell *et al.*, 2002; Guidry & Chafetz, 2003a), where they are composed mainly of opaline silica and/or calcite, in evaporitic playa lakes where they are composed of salts such as gypsum and halite (Renaut *et al.*, 1999), and in dilute lakes undergoing freezing that produce lilypads and ledges of ice. Although influenced by microbial processes, including the development of some microbial fabrics, most lilypads described to date have been attributed to abiotic origins with mineral precipitation induced by either physical or chemical processes that take place at or near the air–water interface (Renaut *et al.*, 1999). The Frying Pan Lake lilypads, however, are clearly of microbial origin, with the framework for the structures being composed entirely of microbial filaments that are templates for silica precipitation.

The growth pattern of the stromatolites can be inferred from observations of the modern examples in different stages of development, and from an examination of the mound structure. Some mounds rise initially from the benthic mat to form small club-shaped columns. Other mounds rise where the mat drapes over protrusions on the substrate such as gravel clasts. Commonly, mats begin to grow over domal highs in the mat itself, forming cabbage-like clumps of mat. Upward growth of the incipient columns then takes place. Some flex and bend, locally becoming detached from the substrate while small, but others continue to grow both upwards and outwards, expanding the diameter of the column. The columns eventually reach the mean water level in the lake. At this point, vertical growth effectively ceases unless the water level rises. Lateral expansion continues, but the rate of expansion is much greater at water level than around the submerged part of the column. This outward growth facilitates the formation of the tabular lilypad plate.

Modern microbial mats formed of *Phormidium* are commonly characterized by columns that are linked by vertical sheets and bridges (Walter *et al.*, 1976; Love *et al.*, 1983; Walter, 1983; Jones *et al.*, 2002). Such mats grow in hot springs at Yellowstone National Park, where temperature is 32–59 °C and pH 7–9 (Walter *et al.*, 1976), and ice-covered lakes of Antarctica where temperature is < 9 °C (Love *et al.*, 1983). In New Zealand, two modern hot springs at Tokaanu have coniform *Phormidium* mats, and fossil examples are present at Whakarewarewa (Jones *et al.*, 2002).

Although several hypotheses have been proposed, the reason(s) as to why columns commonly

Fig. 8. SEM photomicrographs of U-laminae from stromatolite in outflow channel from Frying Pan Lake. (A) General view of upright filaments of *Phormidium*. (B) Silicified *Phormidium* from U-laminae. (C) Silicified epiphytes on surface of silicified sheath shown in (B). (D) Oblique transverse view of U-laminae showing erect *Phormidium* surrounded by opal-A precipitates and various epiphytes including small-diameter filamentous microbes. (E) Tranverse cross-section through U-laminae, parallel to depositional surface, showing complex meshwork of opal-A precipitates and epiphytes between the upright filaments of *Phormidium*. (F) Vertical section through U-laminae showing erect filaments of *Phormidium* with associated epiphytes and opal-A precipitate. (G, H) Longitudinal sections through upright filaments of *Phormidium* showing septa.

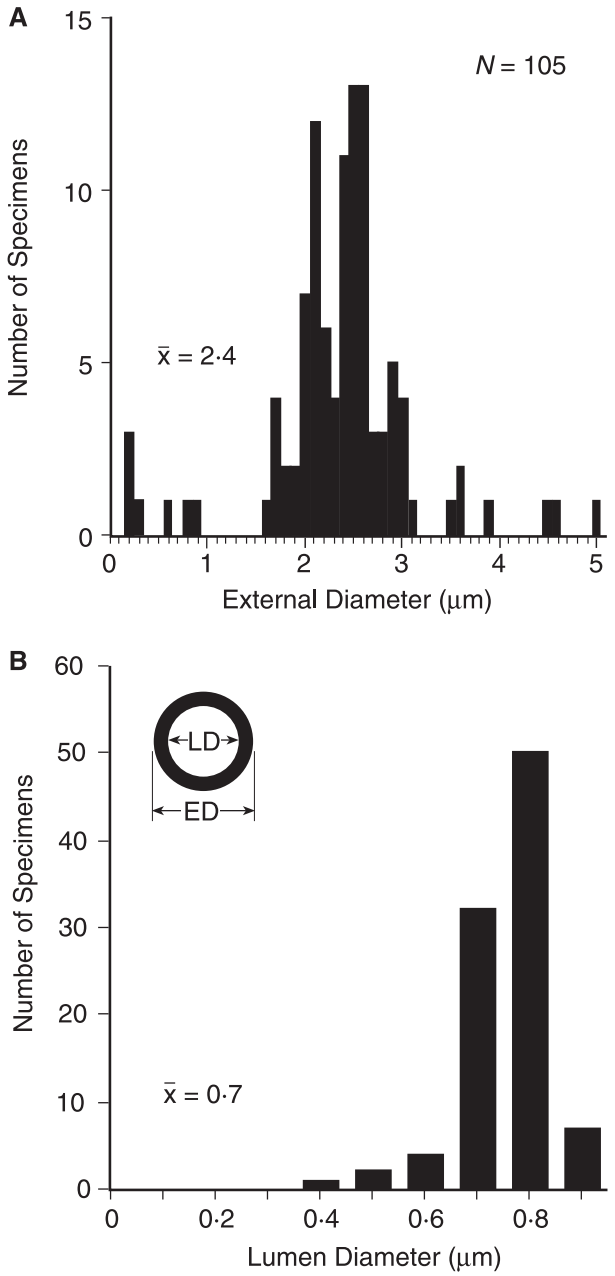

Fig. 9. Frequency distribution histograms for (A) external diameter and (B) internal diameter of filamentous microbes, other than *Fischerella*, from P- and U-laminae in stromatolites from outflow channel of Frying Pan Lake. Measurements to one decimal place derived from SEM photomicrographs.

develop from *Phormidium*-dominated mats is poorly understood. The columns may form as rapidly gliding *Phormidium* filaments become entangled and form small knobs, which then become the preferred habitat for light-seeking microbes (Walter *et al.*, 1976; Awramik & Vanyo, 1983; Walter, 1983). Brock (1978) suggested that column development was promoted by the development of anaerobic conditions in which *Phormidium* thrive, especially where there is a high sulphide content. He argued that the densely interwoven mats promoted anaerobic conditions even in oxygenated water bodies. In contrast, Schultze-Lam *et al.* (1996) and Golubic *et al.* (2000) argued that columnar development in mats formed of tightly interwoven filamentous microbes might be caused by buoyancy that is related to the formation and trapping of gases. Columns growing on the floor of Frying Pan Lake outflow channel may be related to preferential growth on small boulders on the channel floor, and/or local elevation of the microbial mat by gas bubbles constantly escaping from small vents (commonly < 1 cm diameter) on the channel floor. If the model of Brock (1978) is viable, growth of the columns may have also been favoured by the high sulphide content of the water in Frying Pan Lake.

The stromatolites from the Frying Pan Lake outflow channel, like the coniform stromatolites from Kirihoro (Tokaanu), and Waikite Pool, and Te Anarata (Whakarewarewa), are dominated by *Phormidium*. The Frying Pan Lake stromatolites, however, differ from the Tokaanu and Whakarewarewa examples by: (i) being considerably larger, (ii) their development of the lilypad surface, and (iii) generally lacking the vertical sheets and bridges that connect the gaps between neighbouring columns. Nonetheless, some poorly developed drapes extend from some of the columns in the outflow channel from Frying Pan Lake. The currents and high local turbulence may prevent development of large drapes between neighbouring columns. Almost all reported examples of coniform stromatolites with drapes are found in low-energy waters.

Most stromatolites that grow in open lacustrine environments, where water levels remain relatively stable, do not form lilypads even where rapidly mineralized. The specific conditions that promote lilypad development in Frying Pan Lake are unclear. However, the dominance of *Phormidium* may be an important factor in their development. The dense meshwork of filaments constructed by *Phormidium* (Figs 5–8) facilitates columnar growth by providing some rigidity to the developing column even when poorly mineralized. Significantly, even in quiet pools, columnar (coniform) stromatolites develop with *Phormidium*, but the lower energy conditions also allow column linkage by ornate drapery and webbing. In the more agitated waters of Frying

Pan Lake and its outflow channel, extracellular cementation and the binding by epiphytes enhance the strength of the dense meshwork of filaments (Figs 5–8). The cementation initially allows some flexibility, but eventually the columns become more rigid as cementation proceeds. This rigidity, imparted by the meshwork and early mineralization, may allow the mats to grow upwards to the air–water interface, even in energy conditions that would be too high for columns and mats built by other genera. Lateral growth at the air–water interface may then be enhanced by mineralization induced by cooling of the silica-rich fluids and wicking, both of which would reinforce the rigidity of the lilypad plate and increase its resistance to high-energy currents.

The 'lilypad' element of the stromatolites in the Frying Pan Lake outflow channel develops in response to a significant change in the growth dynamics of the stromatolite. The pads, which are characterized by a raised outer rim and a flat interior that is covered by a red-orange microbial mat, formed as the microbial mats spread laterally, at water level, from the top of the columns (Fig. 3). The development of these pads had two significant impacts on the growth dynamics of the stromatolites.

- The overhangs, which are widest on the downstream side, shield the parent column from direct sunlight with the extent of shading depending on the angle of the sun and the width of the overhang (Fig. 3). This shade, in turn, likely reduces rates of photosynthesis and lateral growth of the column compared to the upper surface of the stromatolites, thereby maintaining the mushroom-shaped morphology.
- The microbial mat on the surface of the lilypad grows in an environment that is significantly different from the sub-aqueous environment in which the columns grew. The surface mat is formed of a raised rim, which is in direct contact with the water that is flowing through the channel, and the flat interior that is isolated from the surrounding channel waters (Fig. 3). The interior of the lilypad can become flooded because of: (i) an increase in water level, (ii) wind-generated waves that crest over the peripheral rim, (iii) periods of heavy rain, and (iv) wicking of water through the microbial mat. The depth of water trapped on the lilypad surface is controlled by the volume of water washed onto it and the height of the raised peripheral rim. Water is lost from the surface of the lilypad plate as evaporation takes place. It is unlikely, however, that the mat on the interior of the lilypad will ever dry out to the extent that it will be fully desiccated unless a major fall in water level occurs. Pieces of floating mat are commonly washed onto the surface of the lilypads (Fig. 2E).

One of the most notable features of the lilypad stromatolites is the distinctive red-orange colour of the microbial mat that covers the interior of the lilypad (Fig. 2). Similar colours are evident in some of the *Phormidium*-dominated coniform stromatolites actively growing in an unnamed hot-spring pool opposite Takarea in the Tokaanu geothermal area, which is located at the south end of Lake Taupo (Fig. 1A). Variable colours seem to be a feature of *Phormidium*-dominated microbial mats in many hot-spring systems (Davis, 1897; Copeland, 1936). Orange Mound in Yellowstone National Park, for example, derived its name from the orange colour of the *Phormidium*-dominated microbial mats that cover its surface (Copeland, 1936). Similarly, orange mats dominated by *Phormidium* have been reported from Steep Cone Hot Spring in Yellowstone National Park (Inagaki *et al.*, 2001). Orange bacterial colonies, along with black and green bacterial colonies, have also been reported from lilypad stromatolites that grow in Cistern Spring in Yellowstone National Park (Guidry & Chafetz, 2003a). The colour of such mats, which depends mainly on the ratio of chlorophyll to carotenoids, commonly reflects seasonal changes in microbe growth (e.g. Wiegert & Fraleigh, 1972; Brock, 1994). Thus, the mat will be dark green when low light levels (e.g. during winter) are prevalent. Conversely, during periods of high light levels and high UV radiation, the mats become orange-yellow as the carotenoid pigments increase (Wiegert & Fraleigh, 1972).

An unusual feature of the Frying Pan Lake stromatolites is the pyrite framboids in the M-laminae. Pyrite framboids, found in many different settings, have been attributed to various abiotic and biotic processes (Popa *et al.*, 2004) that include pyritization of individual bacteria or bacterial colonies (Schneiderhohn, 1923; Love, 1957), pyritization of organic particles or colloids (Papunen, 1966; Kalliokoski & Cathles, 1969; Kribek, 1975; Raiswell *et al.*, 1993), low abiotic transformations in Fe–S systems (Rust, 1935; Berner, 1969; Sweeney & Kaplan, 1973; Wilkin & Barnes, 1997), and oxidation of aqueous iron monosulphide by H_2S (Butler & Rickard, 2000). Although Inagaki *et al.* (2001) found pyrite

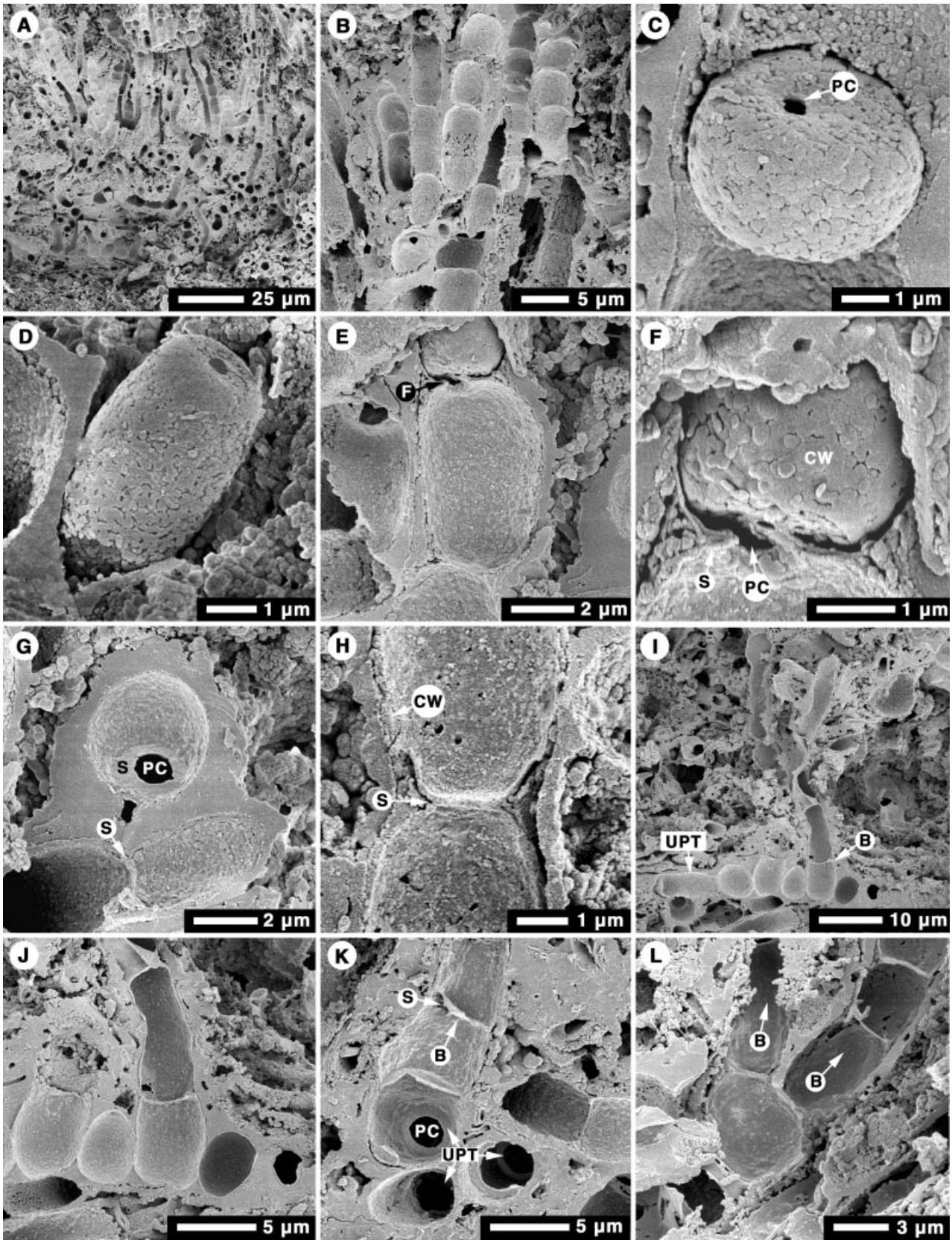
A
25 µm
B
5 µm
C
PC
1 µm
D
1 µm
E
F
2 µm
F
CW
S
PC
1 µm
G
S
PC
S
2 µm
H
CW
S
1 µm
I
UPT
B
10 µm
J
5 µm
K
S
B
PC
UPT
5 µm
L
B
B
3 µm

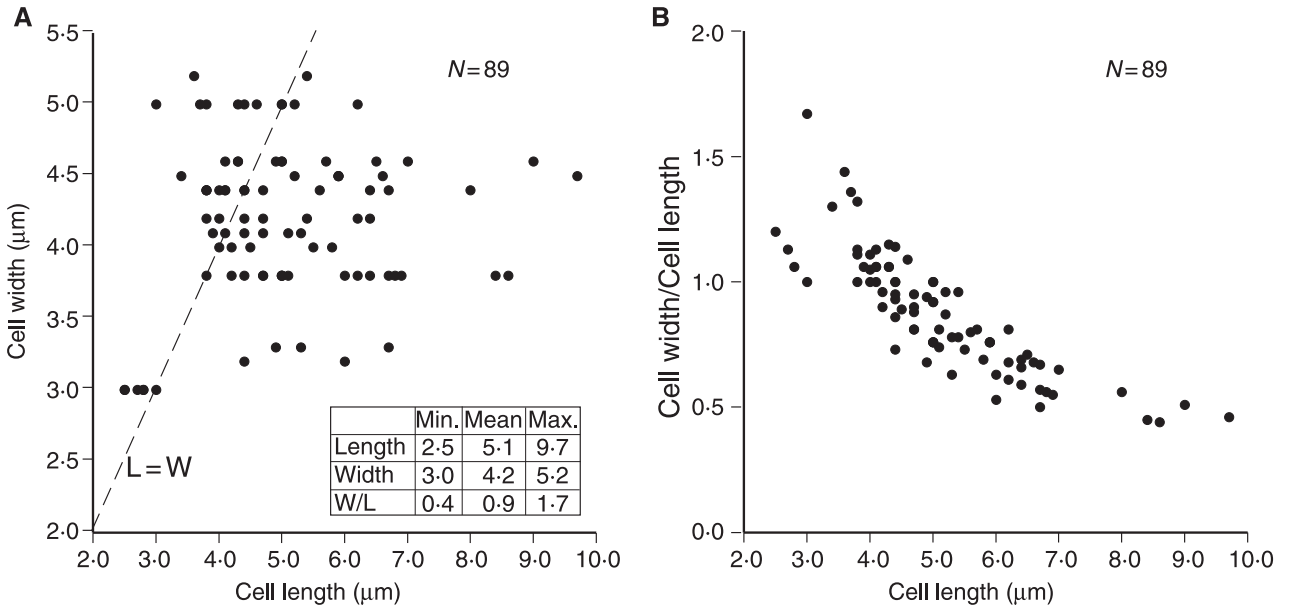

Fig. 11. Bivariant graphs comparing (A) cell length and cell width and (B) cell length and cell width/cell length ratio. The minimum, mean, and maximum for each parameter are given in table. All measurements to one decimal place determined from SEM photomicrographs.

framboids associated with opal-A precipitates in Steep Cone Hot Spring (Yellowstone National Park), they neither described its relationship to the opal-A sinter nor explained its origin. Guidry & Chafetz (2003b) found small (8–40 μm) pyrite framboids inside relict organic remains found in interval 3 (6·8–11·2 m) of core Y-2 from Yellowstone National Park. Hampton *et al.* (2004) reported pyrite framboids (up to 20 μm diameter) in massive and stromatolitic Pliocene sinters at Northland on the North Island of New Zealand. They suggested that the framboids might have formed as a co-precipitate with colloidal silica (Luther *et al.*, 1982) or by replacement of microbial material (Ramdohr, 1969). Pyrite framboids found in aphotic microbial mats in Movile Cave and Buncar Spring, Romania (Popa *et al.*, 2004) were attributed to a two-stage process (Fe monosulphide precipitate replaced by pyrite) that took place under anaerobic conditions within microbial mats. Popa *et al.* (2004) showed that these framboids had few microcrystallites (10–100) compared with abiotic pyrite framboids that contain up to 10^9 microcrystallites. The pyrite framboids in the Frying Pan Lake stromatolites, which are characterized by low numbers of microcrystallites, may have formed in a manner similar to that of the Romanian framboids because they are restricted to the mucus-rich diatom (?) mats that were periodically established on the surfaces of the stromatolites. The extracellular mucus may have facilitated pyrite formation by limiting access to the oxygen produced during photosynthesis.

The growth of stromatolites is controlled by many different variables that are a function of local water and climatic conditions. Indeed, the internal laminations of stromatolites have

Fig. 10. SEM photomicrographs of *Fischerella*. (A) Vertical cross-section through laminae formed of *Fischerella*. (B) Small tuft formed of secondary trichomes of *Fischerella*. (C) Short cylindrical cell pierced by pore channel (PC). (D) Elongate barrel-shaped cell with pore channel (PC). (E) Longitudinal cross-section through trichome showing elongate cell separated by septa. 'F' indicates position of (F). (F) Cell with pore connection abutted against septa (S) that is pierced by open hole (PC). (G) Transverse cross-section through trichome showing septa (S) pierced by pore connection (PC). (H) Longitudinal cross-section through trichome showing elongate cells, silicified cell wall (CW), and septa (S). (I) Uniseriate primary trichome (UPT) resting on depositional surface. Note rotation of cells from which vertical branch (B) originates. (J) Enlarged view of secondary trichome branching from uniseriate primary trichome. (K) Transverse cross-sections through three uniseriate primary trichomes (UPT) and longitudinal cross-section through branch (B – white arrow indicates growth direction); S = septa; PC = pore connection. (L) Two secondary trichomes (branches, B with arrow indicating growth direction) originating from same subspherical cell in uniseriate primary trichome.

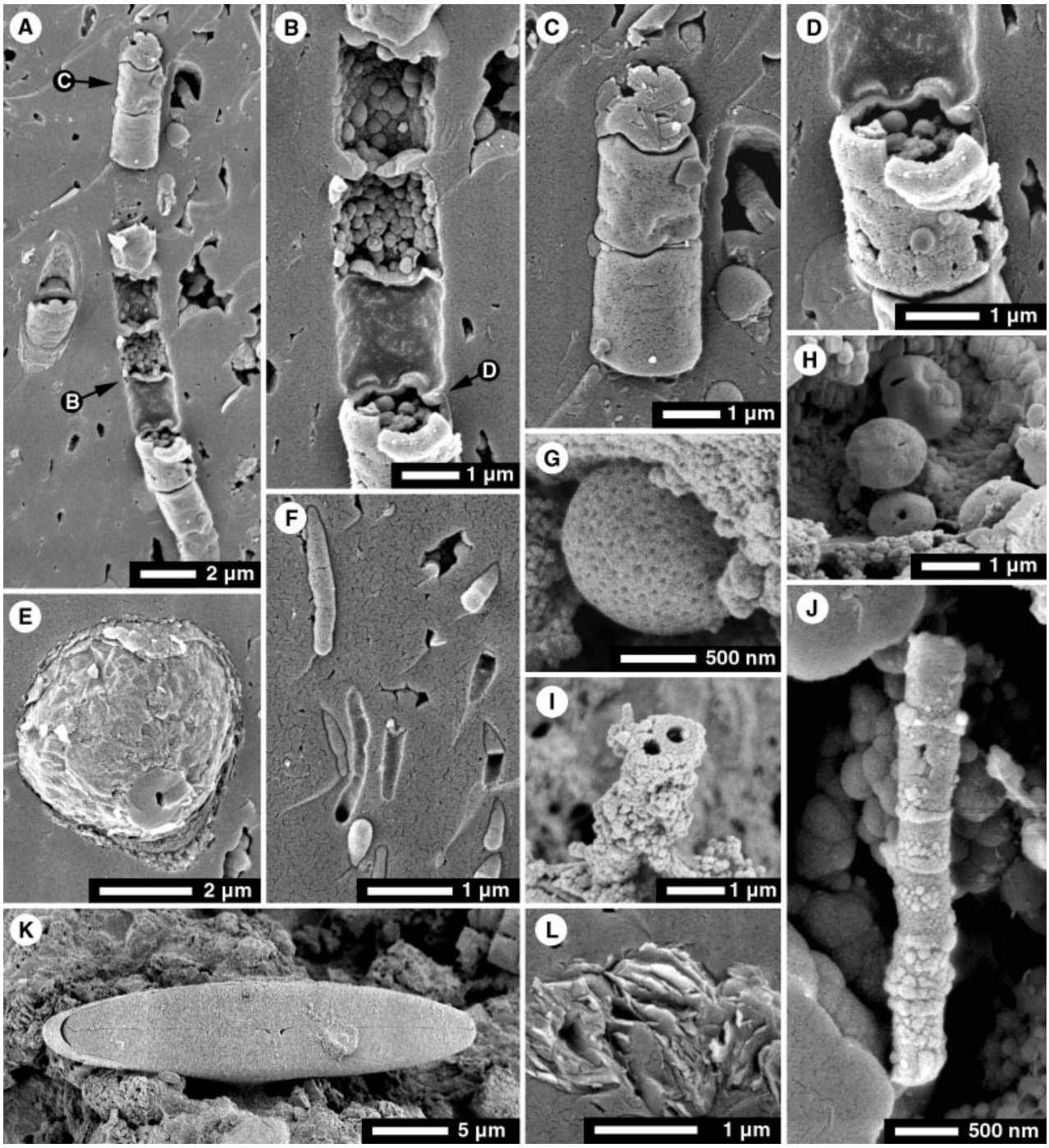

Fig. 12. SEM photomicrographs of microbes that form < 5% of microbiota found in stromatolites from outflow channel from Frying Pan Lake. (A–D) Septate filament. White letters 'B', 'C', and 'D' indicate locations of (B), (C), and (D). (E) Spore of unknown affinity. Note connecting neck with small opening. (F) Small diameter filaments embedded in opal-A matrix. (G, H) Perforate spores of unknown affinity. (I) Two small-diameter filaments merged by silicification. (J) Small-diameter septate filament of unknown affinity. (K) Pennate diatom. (L) Kaolinite embedded in opal-A matrix.

commonly been attributed to time-dependent cyclic variations in these environmental conditions. Information derived from the Frying Pan Lake stromatolites clearly shows that the textures of their internal laminations are related to environmental conditions and that the cycles of P-, U-, and M-laminae, must be related to some aspect of the environment that are subject to cyclic changes.

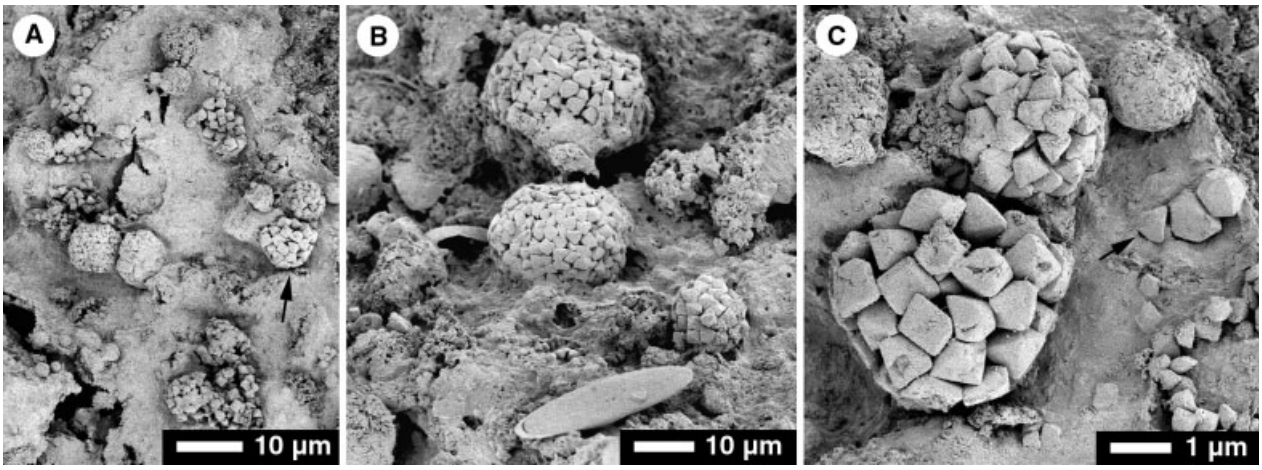

Fig. 13. SEM photomicrographs of M-laminae that commonly overlie the U-laminae. (A) General view of surface showing numerous pyrite framboids embedded in mucus. (B) Pyrite framboids and pennate diatom embedded in mucus. (C) Enlarged view of pyrite framboids and broken framboids embedded in mucus.

Equally, however, it is difficult to relate those laminae to specific environmental parameters.

CONCLUSIONS

The large (3 m × 1 m × 0·5 m), lilypad stromatolites forming around the margins of Frying Pan Lake are constructed mainly by *Phormidium* spp. They form in acidic (pH: 5·6–5·8) hot (48–52 °C) waters on shallow littoral platforms and along the proximal margins of the outflow channel. Columns grow upwards from a thick green benthic mat until they reach the air–water interface, and are succeeded by lateral outgrowth that forms the flat lilypad plate. Enlargement of the plate shades the underlying column, restricting photosynthesis and reducing lateral expansion of the column. The mat community that forms the surficial plate is more diverse than that in the column, with alternating prostrate and erect laminae, and laminae rich in extracellular gels, possibly secreted by diatoms. This diversity reflects the more variable ecological conditions at the water surface, including periodic minor changes in water level. Framboidal pyrite has formed under reducing conditions in the surficial gels.

The unusual growth morphology may reflect the dense meshwork of the *Phormidium* colonies and early partial silicification, which together provide sufficient rigidity to enable the columns to grow well in higher energy conditions than those of most other stromatolites. The lilypad morphology contrasts with the coniform stromatolites produced by *Phormidium*-dominated communities in low-energy hot-spring pools.

ACKNOWLEDGEMENTS

We thank the Natural Sciences and Engineering Research Council of Canada, who funded this research (grants A6090 to B.J.; GP0000629 to R.W.R.; 249565-02 to K.O.K.); Mr Harvey James, CEO for the Waimangu Volcanic Valley, who kindly gave us permission to collect the samples; Mr Ray Wheeler, who helped in the field; Mr George Braybrook (University of Alberta), who took most of the SEM photomicrographs used in this study; and Drs H. Chafetz and K. Campbell who provided critical reviews of an earlier version of this paper. K. Campbell is also acknowledged for communications on storms and high rainfall events leading to fragmentation of mats. Fieldwork was undertaken with the full cooperation and permission of the Department of Conservation, New Zealand, which granted access to the site and allowed the collection of samples. We are very grateful for their continuing support.

REFERENCES

Awramik, S.M. and **Vanyo, J.P.** (1983) Heliotropism in modern stromatolites. *Science*, **231,** 1279–1281.

Bartley, J.K. (1996) Actualistic taphonomy of cyanobacteria: implications for the Precambrian fossil record. *Palaios*, **11,** 571–586.

Berner, R.A. (1969) The synthesis of framboidal pyrite. *Econ. Geol.*, **64,** 383–384.

Brock, T.D. (1978) *Thermophilic Microorganisms and Life at High Temperatures*. Springer-Verlag, New York, 465 pp.

Brock, T.D. (1994) *Life at High Temperatures*. Yellowstone Association for Natural Science, History & Education, Inc., Wyoming, 31 pp.

Brock, T.D. and **Brock, M.** (1970) The algae of Waimangu Cauldron (New Zealand): distribution in relation to pH. *J. Phycol.*, **6,** 371–375.

Brock, T.D. and **Brock, M.** (1971) Microbiological studies of thermal habitats of the central volcanic region, North Island, New Zealand. *N.Z. J. Mar. Freshwat. Res.*, **5,** 233–258.

Butler, I.B. and **Rickard, D.** (2000) Framboidal pyrite formation via the oxidation of iron (II) monosulfide by hydrogen sulphide. *Geochim. Cosmochim. Acta*, **64,** 2665–2672.

Campbell, K.A., Rogers, K.A., Brotheridge, J.M.A. and **Browne, P.R.L.** (2002) An unusual modern carbonate-silica sinter from Pavlova spring, Ngatamariki, New Zealand. *Sedimentology*, **49,** 727–746.

Cassie, V. (1989) A taxonomic guide to thermally associated algae (excluding diatoms) in New Zealand. *Bibliotheca Phycol.*, **38,** 161–255.

Castenholz, R.W. (1969) Thermophilic blue-green algae and the thermal environment. *Bacteriol. Rev.*, **33,** 476–504.

Castenholz, R.W. (1973) Ecology of blue-green algae in hot springs. In: *The Biology of Blue-Green Algae* (Eds N.G. Carr and B.A. Whitton), pp. 379–414. Blackwell Scientific Publications, Oxford.

Castenholz, R.W. (1976) The effect of sulfide on the bluegreen algae of hot springs. I. New Zealand and Iceland. *J. Phycol.*, **12,** 54–68.

Castenholz, R.W. (1978) The biogeography of hot spring algae through enrichment cultures. *Mitt. Int. Verein. Limnol*, **21,** 296–315.

Castenholz, R.W., Rippka, R., Herdman, M. and **Wuilmotte, A.** (2001) Form-genus V. Leptolyngbya Anagnostidis and Komarek, 1988. In: *Bergey's Manual of Systematic Bacteriology*, 2nd edn, Vol. 1 (Eds D.R. Boone and R.W. Castenholz) pp. 544–545. Springer-Verlag, New York.

Caudwell, C., Lang, J.C. and **Pascal, A.** (2001) Lamination of swampy-rivulets *Rivularia haematites* stromatolites in a temperate climate. *Sed. Geol.*, **143,** 125–147.

Chafetz, H.S. and **Folk, R.L.** (1984) Travertines: depositional morphology and the bacterially constructed constituents. *J. Sed. Petrol.*, **54,** 289–316.

Chafetz, H.S., Utech, N.M. and **Fitzmaurice, S.P.** (1991) Differences in the $\delta^{13}O$ and $\delta^{13}C$ signatures of seasonal laminae comprising travertine stromatolites. *J. Sed. Petrol.*, **61,** 1015–1028.

Copeland, J.J. (1936) Yellowstone thermal Myxophyceae. *Annals N. Y. Acad. Sci.*, **36,** 1–229.

Davis, B.M. (1897) The vegetation of the hot springs in Yellowstone Park. *Science*, **6,** 145–157.

Freytet, P. and **Plet, A.** (1996) Modern freshwater microbial carbonates: the *Phormidium* stromatolites (tufa-travertine) of southeastern Burgundy (Paris Basin, France). *Facies*, **34,** 219–238.

Glover, R.B., Stewart, M.K., Crump, M.E., Klyen, L.E. and **Simmons, S.F.** (1994) The relationship of chemical parameters to the cyclic behaviour of Inferno Crater Lake, Waimangu, New Zealand. *Geothermics*, **23,** 583–597.

Golubic, S. and **Focke, J.W.** (1978) *Phormidium hendersonii* Howe: identity and significance of a modern stromatolite building micro-organism. *J. Sed. Petrol.*, **48,** 761–764.

Golubic, A., Seong-Joo, L. and **Browne, K.M.** (2000) Cyanobacteria: architects of sedimentary structures. In: *Microbial Sediments* (Eds R.E. Riding and S.M. Awramik), pp. 57–67. Springer-Verlag, Berlin.

Gonzalez, L.A. and **Lohmann, K.C.** (1988) Controls on mineralogy and composition of spelean carbonates: Carlsbad Caverns, New Mexico. In: *Paleokarst* (Eds N.P. James and P.W. Choquette), pp. 81–101. Springer, New York.

Grange, L.L. (1937) The geology of the Rotorua-Taupo subdivision. New Zealand *Department of Scientific and Industrial Research Bulletin* **37,** 105 p.

Guidry, S.A. and **Chafetz, H.S.** (2003a) Anatomy of siliceous hot springs: examples from Yellowstone National Park, Wyoming, USA. *Sed. Geol.*, **157,** 71–106.

Guidry, S.A. and **Chafetz, H.S.** (2003b) Depositional facies and diagenetic alteration in a relict siliceous hot-spring accumulation: examples from Yellowstone National Park, U.S.A. *J. Sed. Petrol.*, **73,** 806–823.

Hampton, W.A., White, G.P., Hoskin, P.W.O., Browne, P.R.L. and **Rodgers, K.A.** (2004) Cinnabar, livingstonite, stibnite and pyrite in Pliocene silica sinter from Northland, New Zealand. *Mineral. Mag.*, **68,** 191–198.

Hill, C.A. and **Forti, P.** (1997) *Cave Minerals of the World*, 2nd edn. National Speleological Society, Huntsville, AL.

Hindák, F. (2001) Thermal microorganisms from a hot spring on the coast of Lake Bogoria, Kenya. *Nova Hedwigia Beiheft*, **123,** 77–93.

Hoffmann, L. and **Castenholz, R.W.** (2001) Form-genus II. Fischerella Gomont, 1895. In: *Bergey's Manual of Systematic Bacteriology*, 2nd edn, Vol. 1 (eds D.R. Boone and R.W. Castenholz) pp. 593–595. Springer-Verlag, New York.

Hofman, H.J. (1969) Attributes of stromatolites. *Geol. Surv. Can. Pap.*, **69–39,** 1–58.

Houghton, B. and **Scott, B.** (2002) Geyserland – a guide to the volcanoes and geothermal areas of Rotorua. *Guidebook Geol. Soc. N.Z.*, **13,** 48.

Hunt, T.M. (1997) Mitigating the impact of geothermal development: an example from New Zealand. *Chishitsu News*, **8,** 37–42 [in Japanese].

Hunt, T.M, Glover, R.B. and **Wood, C.P.** (1994) Waimangu, Waiotapu, and Waikite geothermal systems, New Zealand: background and history. *Geothermics*, **23,** 379–400.

Inagaki, F., Motomura, Y., Doi, K., Taguchi, S., Izawa, E., Lowe, D.R. and **Ogata, S.** (2001) Silicified microbial community at Steep Cone hot spring, Yellowstone National Park. *Microbes Environ.*, **16,** 125–130.

Joergensen, B.B. and **Nelson, D.C.** (1988) Bacterial zonation, photosynthesis, and spectral light distribution in hot spring microbial mats of Iceland. *Microbial Ecol.*, **16,** 133–147.

Jones, B. and **Kahle, C.F.** (1986) Dendritic calcite crystals formed by calcification of algal filaments in a vadose environment. *J. Sed. Pet.*, **56,** 217–227.

Jones, B., Renaut, R.W. and **Rosen, M.R.** (1997) Vertical zonation of biota in microstromatolites associated with hot springs, North Island, New Zealand. *Palaios*, **12,** 220–236.

Jones, B., Renaut, R.W. and **Rosen, M.R.** (1998) Microbial biofacies in hot-spring sinters: a model based on Ohaaki Pool, North Island, New Zealand. *J. Sed. Res.*, **68,** 413–434.

Jones, B., Renaut, R.W. and **Rosen, M.R.** (1999) Actively growing siliceous oncoids in the Waiotapu geothermal area, North Island, New Zealand. *J. Geol. Soc. London*, **156,** 89–103.

Jones, B., Renaut, R.W. and **Rosen, M.R.** (2000) Stromatolites forming in acidic hot-spring waters, North Island, New Zealand. *Palaios*, **15,** 450–475.

Jones, B., Renaut, R.W. and **Rosen, M.R.** (2001) Taphonomy of silicified filamentous microbes in modern geothermal sinters – implications for identification. *Palaios*, **16,** 580–592.

Jones, B., Renaut, R.W., Rosen, M.R. and **Ansdell, K.M.** (2002) Coniform stromatolites from geothermal systems, North Island, New Zealand. *Palaios*, **17,** 84–103.

Jones, B., Renaut, R.W. and **Rosen, M.R.** (2004) Taxonomic fidelity of silicified microbes from hot spring systems in the Taupo Volcanic Zone, North Island, New Zealand. *Phil. Trans. R. Soc. Edinb. Earth Sci.*, **94,** 475–484.

Kalliokoski, J. and **Cathles, L.** (1969) Morphology, mode of formation and diagenetic changes in framboids. *Bull. Geol. Soc. Finland*, **41,** 125–133.

Kano, A., Matsuoka, J., Kojo, T. and **Fujii, H.** 2003. Origin of annual laminations in tufa deposits, southwest Japan. *Palaeogeogr. Palaeoclimatol. Palaeoecol.*, **191,** 243–262.

Keam, R.F. (1955) *Volcanic Wonderland. The Scenery and Spectacle of the New Zealand Thermal Region*. G.B. Scott, Auckland, 49 pp.

Keam, R.F. (1981) Frying Pan Lake – provisional bathymetry 1:250. Misc. Ser. 53, New Zealand Oceanography Institute, Wellington.

Konhauser, K.O., Phoenix, V.R., Bottrell, S.H., Adams, D.G. and **Head, I.M.** (2001) Microbial-silica interactions in Icelandic hot spring sinter: possible analogues for some Precambrian siliceous stromatolites. *Sedimentology*, **48,** 415–433.

Kribek, B. (1975) The origin of framboids as a surface effect on sulphur grains. *Mineral. Depos.*, **10,** 389–396.

Lloyd, E.F. (1973) Geothermal observations, 1971. Waimangu. *N.Z. Volcanol. Rec.*, **1,** 34–37.

Lloyd, E.F. (1974) Waimangu hydrology and temperature measurements – 1972. *N.Z. Volcanol. Rec.*, **2,** 55–57.

Lloyd, E.F. and **Keam, R.F.** (1974) Trinity Terrace hydrothermal eruption, Waimangu, New Zealand. *N.Z. J. Sci.*, **17,** 511–528.

Love, L.G. (1957) Micro-organisms and the presence of syngenetic pyrite. *Q. J. Geol. Soc. London*, **113,** 429–440.

Love, F.G., Simmons, G.M., Parker, B.C., Wharton, R.A. and **Seaburg, K.G.** (1983) Modern Conophyton-like microbial mats discovered in Lake Vanda, Antarctica. *Geomicrobiol. J.*, **3,** 33–48.

Luther, G.W., Giblin, A., Howarth, R.W. and **Ryans, R.A.** (1982) Pyrite and oxidised iron mineral phases formed from pyrite oxidation in salt marsh and estuarine sediments. *Geochim. Cosmochim. Acta*, **46,** 2665–2669.

Mahon, W.A.J. (1965) Waimangu geochemistry. *N.Z. Dept. Sci. Indust. Res., Volcanol. Inform. Ser.*, **50,** 46–48.

Mann, A.W., Fardy, J.J. and **Hedenquist, J.W.** (1986) Major and trace element concentrations in some New Zealand geothermal waters. In: *Proceedings of Symposium 5: Volcanism, hydrothermal systems and related mineralization*, International Volcanological Congress, p. 61–66.

Merz, M.U.E. (1992) The biology of carbonate precipitation by Cyanobacteria. *Facies*, **26,** 81–101.

Monty, C.L.V. (1967) Distribution and structure of recent stromatolitic algal mats, eastern Andros Island, Bahamas. *Annal. Soc. Géol. Belg.*, **96,** 585–624.

Monty, C.L.V. (1976) The origin and development of cryptalgal fabrics. In: *Stromatolites (Developments in Sedimentology 20)* (Ed. M.R. Walter) pp. 193–250. Elsevier, Amsterdam.

Nash, A. (1938) *The cyanophyceae of the thermal regions of Yellowstone National Park, U.S.A., and Rotorua and Whakarewarewa, New Zealand; with some ecological data*. PhD thesis, University of Minnesota, Minneapolis.

Papunen, H. (1966) Framboidal textures of the pyritic layer found in a peat bog in S.E. *Finland. Bull. Comm. Géol. Finlande*, **222,** 117–125.

Park, R. (1976) A note on the significance of lamination in stromatolites. *Sedimentology*, **23,** 379–393.

Phoenix, V.R., Adams, D.G. and **Konhauser, K.O.** (2000) Cyanobacterial viability during hydrothermal biomineralization. *Chem. Geol.*, **169,** 329–338.

Popa, R., Kinkle, B.K. and **Badescu, A.** (2004) Pyrite framboids as biomarkers for iron-sulfur systems. *Geomicrobiol. J.*, **21,** 193–206.

Raiswell, R., Whaler, K., Dean, S., Coleman, M.L. and **Briggs, D.E.G.** (1993) A simple three–dimensional model of diffusion with precipitation applied to localised pyrite formation in framboids, fossils and detrital iron minerals. *Mar. Geol.*, **113,** 89–100.

Ramdohr, P. (1969) *The Ore Minerals and their Intergrowths*. Pergamon, London.

Renaut, R.W., Jones, B. and **Rosen, M.R.** (1996) Primary silica oncoids from Orakeikorako hot springs, North Island, New Zealand. *Palaios*, **11,** 446–458.

Renaut, R.W., Jones, B. and **Le Turdu, C.** (1999) Calcite lily-pads and ledges at Lorusio Hot Springs, Kenya Rift Valley: travertine precipitation at the air-water interface. *Can. J. Earth Sci.*, **36,** 649–666.

Riding, R. (1991) Calcified Cyanobacteria. In: *Calcareous Algae and Stromatolites* (Ed. R. Riding) pp. 55–87. Springer Verlag, Berlin.

Rippka, R., Deruelles, J., Waterbury, J.B., Herdman, M. and **Stanier, R.Y.** (1979) Generic assignments, strain histories and properties of pure cultures of Cyanobacteria. *J. Gen. Microbiol.*, **111,** 1–61.

Rust, G.W. (1935) Colloidal primary copper ores at Cornwall Mines, Missouri. *J. Geol.*, **43,** 398–426.

Schneiderhohn, H. (1923) Chalkographische untersuchung des Mansfelder Kupferscheifers. *N. Jahrb. Geol. Paläontol. Abhand.*, **47,** 1–38.

Schultze-Lam, S., Ferris, F.G., Sherwood-Lollar, B. and **Gerits, J.P.** (1996) Ultrastructure and seasonal growth patterns of microbial mats in a temperate climate saline-alkaline lake: Goodenough Lake, British Columbia, Canada. *Can. J. Microbiol.*, **42,** 147–161.

Scott, B.J. (1992) *Waimangu: a volcanic encounter. Waimangu Volcanic Valley, Rotorua, New Zealand*.

Scott, B.J. (1994) Cyclic activity in the crater lakes of Waimangu hydrothermal system, New Zealand. *Geothermics*, **23,** 555–572.

Seward, T.M. and **Sheppard, D.S.** (1986) Waimangu geothermal field. In: *Guide to the Active Epithermal (Geothermal) Systems and Precious Metal Deposits of New Zealand* (Eds R.W. Henley, J.W. Hedenquist and P.J. Roberts), *Monogr. Ser. Mineral Dep.*, **26,** 81–91.

Sheppard, D.S. (1986) Fluid chemistry of the Waimangu geothermal system. *Geothermics*, **15,** 309–328.

Sweeney, R.E. and **Kaplan, I.R.** (1973) Pyrite framboid formation: laboratory synthesis and marine sediments. *Econ. Geol.*, **68,** 618–634.

Symoens, J.J. (1957) Les eaux douces des Ardennes et des régions viosines: les milieux et leur végétation algale. *Bull. Soc. R. Bot. Belg.*, **89,** 111–314.

Walter, M.R. (1972) A hot spring analog for the depositional environment of Precambrian Iron Formations of the Lake Superior Region. *Econ. Geol.*, **67,** 965–980.

Walter, M.R. (1976) Hot-springs sediments in Yellowstone National Park. In: *Stromatolites (Developments in Sedimentology 20)* (Ed. M.R. Walter) pp. 489–498. Elsevier, Amsterdam.

Walter, M.R. (1983) Archean stromatolites: evidence of Earth's earliest benthos. In: *Earth's Earliest Biosphere* (Ed. J.W. Schopf) pp. 187–213. Princeton University Press, Princeton, NJ.

Walter, M.R., Bauld, J. and **Brock, J.D.** (1972) Siliceous algal and bacterial stromatolites in hot spring and geyser effluents of Yellowstone National Park. *Science*, **178,** 402–405.

Walter, M.R., Bauld, J. and **Brock, T.D.** (1976) Microbiology and morphogenesis of columnar stromatolites (Conophyton, Vacerrilla) from hot springs in Yellowstone National Park. In: *Stromatolites (Developments in Sedimentology 20)* (Ed. M.R. Walter) pp. 273–310. Elsevier, Amsterdam.

Weissberg, B.G. (1969) Gold-silver ore-grade precipitates from New Zealand thermal waters. *Economic Geology*, **64,** 95–108.

White, W.B. (1976) Cave minerals and speleothems. In: *The Science of Speleology* (Eds T.D. Ford and C.H.D. Cullingford) pp. 155–171. Academic Press, London.

Wiegert, R.G. and **Fraleigh, P.C.** (1972) Ecology of Yellowstone thermal effluent systems: net primary production and species diversity of a successional blue-green algal mat. *Limnol. Oceanogr.*, **17,** 215–228.

Wilkin, R.T. and **Barnes, H.L.** (1997) Formation processes of framboidal pyrite. *Geochim. Cosmochim. Acta*, **61,** 323–339.

Manuscript received 14 October 2004;
revision accepted 1 June 2005.